

# Intraseasonal to interannual variability of zooplankton biomass and standing stock inferred from ADCP backscatter in the eastern Arabian Sea

Ranjan Kumar Sahu<sup>a,b</sup>, D. Shankar<sup>a,b,\*</sup>, P. Amol<sup>b,c</sup>, S.G. Aparna<sup>a,b</sup>, D.V. Desai<sup>a,b</sup>

<sup>a</sup>*organization=CSIR-National Institute of Oceanography, addressline=Dona Paula,  
postcode=403004, state=Goa, country=India*

<sup>b</sup>*organization=Academy of Scientific and Innovative Research (AcSIR), addressline=Ghaziabad,  
postcode=201002, state=Uttar Pradesh, country=India*

<sup>c</sup>*organization=CSIR-NIO, Regional Centre, addressline=Visakhapatnam, postcode=530017,  
state=Andhra Pradesh, country=India*

---

## Abstract

The spatio-temporal variation of zooplankton biomass and standing stock in the eastern Arabian Sea (EAS) is mapped using backscatter measurements from 153.3 kHz acoustic Doppler current profiler (ADCP) moorings deployed at seven locations on the continental slope off the west coast of India from October 2017 to December 2023. The conversion from backscatter to biomass is based on volumetric zooplankton sampling. Zooplankton biomass in 24–140 m decreases from the upper ocean to lower depths. Changes are observed in seasonal variation of zooplankton standing stock monthly climatology (24–120 m biomass integral) as we move poleward along the slope. Standing stock variation is lowest at Kanyakumari followed by Okha, each at the southern and northern boundary of EAS, respectively. Analysis reveals weak annual cycle in zooplankton biomass and dominance of intraseasonal and intra-annual components. Annual cycle is predominant at northeastern Arabian

---

\*Corresponding author

Email address: shankar@nio.res.in (D. Shankar)

Sea (NEAS) and it decreases towards southeastern Arabian Sea (SEAS) where the semi-annual cycle tends to dominate. Interannual variability, which is rarely addressed in conventional studies, is observed off Kollam with peaks corresponding to period  $\sim$ 720 days, moderately off Mumbai and feebly off Goa. Intraseasonal variability is often comparable (stronger) to the intra-annual (annual) variability both of which increases (decreases) equatorward with an evident presence in SEAS. Stronger intraseasonal variability has implication on zooplankton sampling using conventional methods, and it's patchiness in open ocean. Further, it also impacts the accurate estimation of standing stock and on reduced predictability of biomass.

*Keywords:* ADCP backscatter, zooplankton, biomass, standing stock, variability, eastern Arabian Sea

---

## 1. Introduction

### 2 1.1. Background

Zooplankton plays a vital role in food web of pelagic ecosystem by enabling the hierarchical transport of organic matter from primary producers to higher trophic levels impacting the fish population (Ohman and Hirche, 2001) and the carbon pump of the deep ocean (Quéré et al., 2016). They are presumably the largest migrating organisms in terms of biomass (Hays, 2003) which occurs in diel vertical migration (DVM). Zooplankton depend not only on phytoplankton but other environmental parameters (e.g. mixed-layer depth, insolation, oxygen, thermocline, nutrient availability, chl-a concentration and daily primary production). The biological productivity of the ocean is essentially connected with physics and chemistry (Subrahmanyam, 1959; Ryther et al., 1966; Nair, 1970; Qasim, 1977; Banse, 1995; McCreary et al., 2009; Vijith et al., 2016; Amol et al., 2020). The dynamic ocean results in varying physico-chemical properties, leading to bloom and growth of plankton in favourable conditions. The changes are strongly influenced by the seasonal cycle in the North Indian Ocean (NIO; north of 5°N of Indian Ocean). The eastern boundary of Arabian Sea contains the West India Coastal Current (WICC; Ramamirtham and Murty, 1965; Banse, 1968; Shetye et al., 1990; McCreary et al., 1993; Amol et al., 2014; Vijith et al., 2016; Chaudhuri et al., 2020) which reverses seasonally, flowing poleward (equatorward) during November to February (June to September) (Shetye et al., 1990, 1991; Vijith et al., 2022).

22 A direct consequence of this reversal is the seasonal cycle of thermocline (Prasad and Bahulayan, 1996; Kumar and Narvekar, 2005), oxycline (DeSousa et al., 1996; Schmidt et al., 2020) and thickness of mixed-layer depth (MLD; Shetye et al., 1991; Prasad and Bahulayan, 1996; Kumar and Narvekar, 2005) induced by upwelling

26 (downwelling) favourable conditions in summer (winter) at eastern Arabian Sea  
27 (EAS) facilitated further by wind speed and near-surface stratification. Further,  
28 the phytoplankton biomass and chl-a concentration changes with the season (Sub-  
29 rahmanyam and Sarma, 1960; Banse, 1968; Kumar and Narvekar, 2005; Lévy et al.,  
30 2007; Vijith et al., 2016). Upwelling in summer monsoon leads to maximum chl-a  
31 growth in the entire EAS (Banse, 1968; Banse and English, 2000; McCreary et al.,  
32 2009; Hood et al., 2017; Bemal et al., 2018; Shi and Wang, 2022). During winter  
33 monsoon, the convective mixing induced winter mixed layer (Shetye et al., 1992;  
34 Madhupratap et al., 1996b; McCreary et al., 1996; Lévy et al., 2007; Shankar et al.,  
35 2016; Vijith et al., 2016; Keerthi et al., 2017; Shi and Wang, 2022) results in winter  
36 chl-a peak at NEAS while the downwelling Rossby waves modulate chl-a along SEAS  
albeit limited to coast and islands (Amol et al., 2020).

38 The zooplankton grazing peak is instantaneous with no time delay from peak  
39 phytoplankton production (Li et al., 2000; Barber et al., 2001), but its population  
40 growth lags (Rehim and Imran, 2012; Almén and Tamelander, 2020) depending on  
41 its gestation period and other limiting aspects. While some studies suggest that the  
42 peak timing of zooplankton may not change in parallel with phytoplankton blooms  
43 (Winder and Schindler, 2004), others indicate that lag exists between primary pro-  
44 duction and the transfer of energy to higher trophic levels (Brock and McClain, 1992;  
45 Brock et al., 1991). The conventional zooplankton measurements, where only few  
46 snapshots of the event is captured gives an incoherent or incomplete understanding in  
47 terms of spatio-temporal variation of zooplankton (Ramamurthy, 1965; Madhupratap  
48 et al., 1992; Piontковski et al., 1995; Madhupratap et al., 1996a; Wishner et al., 1998;  
49 Kidwai and Amjad, 2000; Barber et al., 2001; Khandagale et al., 2022) as much in-  
50 formation is revealed by later studies (Jyothibabu et al., 2010; Shankar et al., 2019;  
Aparna et al., 2022) using high resolution data. Calibrated acoustic instruments

such as acoustic Doppler current profiler (ADCP) along with relevant data can be utilised to understand small scale variability (Nair et al., 1999; Edvardsen et al., 2003; Smith and Madhupratap, 2005; Smeti et al., 2015; Kang et al., 2024), the complex interplay between the physico-chemical parameters and ecosystem (Jiang et al., 2007; Potiris et al., 2018; Shankar et al., 2019; Aparna et al., 2022; Nie et al., 2023), the zooplankton migration (Inoue et al., 2016; Ursella et al., 2018, 2021) and their seasonal to annual variation (Jiang et al., 2007; Hobbs et al., 2021; Liu et al., 2022; Aparna et al., 2022).

The relationship between backscatter and the abundance and size of zooplankton was described by Greenlaw (1979) with single frequency backscatter used to estimate abundance along with knowledge of mean zooplankton size. A drastic increase in study temporal and spatial variation of zooplankton biomass using backscatter-proxy came in 1990s by introduction of high-frequency echo sounders, with studies (Flagg and Smith, 1989; Wiebe et al., 1990; Batchelder et al., 1995; Greene et al., 1998; Rippeth and Simpson, 1998) methodically showing acoustic backscatter estimated zooplankton biomass. Net sampling augmented ADCP backscatter have been used to study DVM and the spatial and temporal variability of zooplankton biomass in different marine regions, such as the Southwestern Pacific, the Lazarev Sea in Antarctica and the Corsica Channel in the north-western Mediterranean Sea (Cisewski et al., 2010; Hamilton et al., 2013; Smeti et al., 2015; Guerra et al., 2019). The first such study to exploit the potential of ADCPs in EAS was carried out by Aparna et al. (2022) (A22 from hereon) using ADCP moorings deployed on continental slopes off the Indian west coast. A22 showed that the zooplankton standing stock (ZSS) in fact declines during upwelling facilitated increase in phytoplankton biomass. The unusual interaction implies the break down of existing understanding of predator-prey relationship in fundamental level of marine food chain.

78    *1.2. Objective and scope of the manuscript*

The network of ADCPs was installed off the continental slope and shelf on the  
80    west coast of India. These ADCPs have enabled a rigorous view of intraseasonal to  
82    seasonal scale variability (Amol et al., 2014; Chaudhuri et al., 2020) of WICC. In the  
84    recent study A22 have used ADCP moorings off Mumbai, Goa and Kollam to explain  
the temporal variability of zooplankton biomass. The study showed that the zooplankton  
86    peaks (and troughs) is not only non-uniform in latitude but also heavily influenced by the oxygen minimum zone, MLD and the seasonal upwelling/downwelling  
88    conditions. Stark contrast in the phytoplankton bloom and subsequence growth of  
zooplankton or the lack thereof was observed in the EAS regimes.

We extend the work of A22 by presenting data from four additional moorings in  
88    the EAS, showcasing the deviations of seasonal cycle from climatology, and discussing  
90    the significant intraseasonal variability of biomass and standing stock revealed by the  
92    ADCP data. The paper is organized as follows; datasets and methods employed are  
described in section 2. Section 3 describes the observed time series, climatology of  
94    zooplankton biomass and standing stock, their seasonal cycle and variability. A brief  
96    discussion on interannual variability in section 4 is followed by a detailed discussion  
in section 5 on intraseasonal variability which is a major focus in this study. We delve  
deeper into the summary, discussions on implications of intraseasonal variability and  
conclusion in section 6.

98    **2. Data and methods**

Backscatter data from ADCP and the zooplankton samples collected from the  
100    periphery of mooring is described in this section. The backscatter derived from the  
echo intensity of the seven ADCP mooring deployed on the continental slope off the

102 Indian west coast is the primary data used. The moorings details are summarized  
104 in [table 1](#). In situ biomass data from volumetric zooplankton samples are used to  
106 validate and correlate with backscatter. The chl-a data is used to study and draw  
inferences for the possible zooplankton growth seasons. In addition, we have used  
the monthly climatology of temperature and salinity from [Chatterjee et al. \(2012\)](#).

### *2.1. ADCP data and backscatter estimation*

108 ADCPs were deployed on the continental slope off the Indian west coast ([Fig. 1](#)),  
110 off Mumbai, Goa, and Kollam, and later extended to additional four sites to cover  
the entire EAS basin from Okha ( $22.26^{\circ}\text{N}$ ) in north to Kanyakumari ( $6.96^{\circ}\text{N}$ ) in  
112 south. The other two ADCPs are, 1) Jaigarh at central EAS (CEAS), 2) Udupi  
(primarily at SEAS regime) in the transition zone between CEAS and SEAS. The  
114 extended moorings were deployed in October 2017, though Kanyakumari had been  
deployed earlier. The moorings are serviced on yearly basis usually during October–  
November or sometime during September–December (depending on ship availability).  
116 The ADCPs are of Teledyne RD Instruments make, upward-looking and operate at  
153.3 kHz. While utmost care is taken to position the instrument (mooring) at  $\sim$ 150–  
118 200 m ( $\sim$ 1050–1100 m) depth, yet for some deployments it's shallow or deeper owing  
to drift caused by floater-buoyancy and anchor-weight imbalance. Data was collected  
120 at hourly interval with 4 m bin size. The echoes at surface to 10% range ( $\sim$ 20 m)  
renders the data useless and is discarded from further use. We have followed the  
122 methodology laid down in A22 to derive the backscatter time series from ADCP echo  
intensity. Gaps up to two days are filled using the grafting method of [Mukhopadhyay  
et al. \(2017\)](#) once the zooplankton biomass time series is constructed.

## *2.2. Zooplankton data and estimation of biomass*

The zooplankton samples were collected in the vicinity ( $\sim 10$  km) of ADCP mooring site twice, once prior retrieval and again post deployment of moorings in order to have an overlap in the ADCP time instance and in situ zooplankton samples during servicing cruises on board of RV Sindhu Sankalp and RV Sindhu Sadhana (table 2). Multi-plankton net (MPN, 100  $\mu\text{m}$  mesh size, 0.5  $\text{m}^2$  mouth area) was used to get samples in the pre-determined depth ranges; water volume filtered was calculated by sampling depth range and mouth area. The depth range and timing of sample collection was different throughout the MPN hauls (refer table 2). From 2020 onward, the depth-range was standardized to the bins of 0–25, 25–50, 50–75, 75–100, 100–150 (units are in meters). Backscatter is averaged in vertical corresponding to the specific bins of MPN haul for each site and then linearly regressed with biomass of respective bins (Fig. 2), as demonstrated in numerous previous studies (Flagg and Smith, 1989; Heywood et al., 1991; Jiang et al., 2007; Aparna et al., 2022). The zooplankton biomass in the euphotic zone concentrate in the upper 10m which is pronounced during night. However, this should not be a concern as it would simply show up as low backscatter at deeper depths during night time corresponding to low biomass. It is important to note that the study is carried out using daily averaged biomass. Therefore, features associated with DVM is eliminated and seasonal cycle (Jiang et al., 2007, A22) which is the major focus of our work can be studied.

### *2.2.1. Biomass time series and estimation of standing stock*

Zooplankton biomass time series (Fig. 3) is created from the above linear regression. Standing stock is determined by taking the depth integral of biomass over the water column. To maintain the consistency of standing stock estimation, only those deployments that does not lack data at any depth in the entire range of 24–120

<sup>150</sup> m are considered for analysis as in A22. The lack of data in the above mentioned  
<sup>151</sup> depth range is due to deviation in positioning of ADCP sensor in the water column.  
<sup>152</sup> Alteration in bathymetry along the continental slope suggests mooring may anchor  
<sup>153</sup> at different depth. It leads to gap in data at few mooring sites for some year. For  
<sup>154</sup> example at Okha, data is not available for the entire upper 120 m depth for the  
<sup>155</sup> second deployment. Also at Jaigarh, where the surface to ~60 m data (in third de-  
<sup>156</sup> ployment) and Kollam, where 80 m and below (in fourth deployment) is unavailable.  
<sup>157</sup> There are few deployments where no data or bad data was recorded e.g, at Udupi  
<sup>158</sup> (fourth deployment) and Kanyakumari (sixth deployment) and hence discarded from  
standing stock estimation.

<sup>160</sup> *2.3. Mixed-layer depth, temperature, oxygen and chlorophyll*

MLD in EAS is of the order ~20 to 40 m during summer monsoon ([Shetye et al., 1990](#); [Shankar et al., 2005](#); [Sreenivas et al., 2008](#)) especially in the SEAS ([Shenoi et al., 2005](#)), but during winter the MLD in northern NEAS remains deep ([Shankar et al., 2016](#)). The temperature data is used from [Chatterjee et al. \(2012\)](#), a monthly climatology having 1° spatial resolution. Monthly climatology of oxygen data is obtained from World Ocean Atlas 2013 ([García et al., 2014](#)) which contains objectively analyzed 1° climatological fields of in situ measurements. Previous study based on ADCP data of EAS A22 have used SeaWiFS based chl-a data for comparison with climatology of ZSS. The SeaWiFS was at its end of service in 2010, hence we use new chl-a product from Global Ocean Colour, biogeochemical L3 data obtained from [E.U. Copernicus Marine Service Information](#). The daily data is available at a spatial resolution of 4 km.

### 3. Time series, climatology and seasonal cycle

174        Monthly climatology of biomass and ZSS is computed for all locations having valid  
175        data in 24–140 m depth range. To distinguish between high and low productivity  
176        zones, we employed a biomass contour, similar to the  $215 \text{ mg m}^{-3}$  threshold used in  
177        A22 but with exception of Kollam during 2020 as variation in the monthly averaged  
178        data suggests presence of strong interannual variability. It is of two distinct types,  
179        1) deviation from the seasonal cycle and is aperiodic, 2) variation associated with  
180        interannual climate modes and it is quasi-periodic. For the years 2019 and 2020 the  
181        low biomass is observed at depths as much as near to the surface regime off Kollam  
182        ([Fig. 3](#)). But for the years 2018, 2022, and 2023 the high biomass occurs at deeper  
183        depths. Since we can't use two contours for demarcating the high biomass for same  
184        time series, we couldn't use any contour for the year 2020 when it is shallowest and  
185        isn't a representative of the seasonal variation.

186        A decrease in biomass with increasing depth at all seven study sites is observed  
187        ([Fig. 3](#)). The demarcating biomass contour (z215) and its depth contour (D215)  
188        allows us to link the seasonal variation of biomass to the physico-chemical proper-  
189        ties. However, to better capture seasonal variations off Kanyakumari and Okha, the  
190        threshold was replaced by  $175 \text{ mg m}^{-3}$ . Time series, climatology and seasonal cycle  
191        of biomass is discussed in the following sections. For a comparison with physico-  
192        chemical forcing, we use isotherm of  $23^\circ\text{C}$  (henceforth, D23) and oxygen contour  
193        specific to each site depending on its position relative to oxygen minimum zone  
194        (OMZ) boundaries of EAS.

#### 3.1. Time series description

196        Rate of biomass decrease with depth, roughly defined as the difference between  
197        mean biomass at 40 and 104 m depth is highest off Jaigarh and Mumbai as it has

<sup>198</sup> higher biomass in upper ocean ([Fig. 4](#)) and lowest off Kanyakumari. This is followed  
<sup>199</sup> by Goa and Udupi. While the biomass decrease with depth is lower off Kollam from  
<sup>200</sup> 2017 to 2020, it becomes considerably high from thereon ([Fig. 4 f](#)). A comparatively  
<sup>201</sup> moderate decline in zooplankton biomass with respect to depth off Okha ([Fig. 3](#)  
<sup>202</sup> a1, a2) at NEAS is agreeing with earlier reported data ([Wishner et al., 1998; Mad-](#)  
<sup>203</sup> [hupratap et al., 2001; Smith and Madhupratap, 2005; Jyothibabu et al., 2010](#)). The  
<sup>204</sup> difference of mean biomass at 40 and 104 m is high at most location but it arises  
due to the bigger difference in select few years, e.g., off Mumbai during 2020 and  
<sup>205</sup> 2022, off Jaigarh in 2021, at Goa during 2021–2022, off Kollam during 2022. The  
sites at SEAS, particularly off Kanyakumari for all years and 2017 to 2020 off Kol-  
<sup>206</sup> lam also have weaker decrease ([Madhupratap et al., 2001; Jyothibabu et al., 2010](#);  
<sup>207</sup> [Aparna et al., 2022](#)). However, the biomass decline with depth post 2021 off Kollam  
<sup>208</sup> is high owing to a strong bloom in these years and is reflected as D215 deepening.  
D175 /D215 is deep throughout EAS during winter monsoon as seen from the same  
<sup>209</sup> biomass value at 40 and 104 m indicating the penetration of D215/D175 all the way  
to 104 m, but the occurrence time of high biomass is distinct to each regime of EAS.  
<sup>210</sup> Upper ocean shows considerably high biomass and ZSS during winter monsoon at  
NEAS. On the contrary at SEAS, the upper ocean shows higher biomass during  
<sup>211</sup> summer monsoon even though the D215 and D175 is shallower during this period.

The mean, standard deviation of biomass, ZSS and chl-a are shown in table S1.  
<sup>212</sup> There is no consistent variation as seen from the analysis of mean and standard  
deviation of biomass at 40 and 104 m. The sites with higher biomass tends to  
<sup>213</sup> have higher variation over time e.g. Mumbai, Jaigarh and Kollam. Superposed on  
the time-series is seasonal cycle and variability of distinct period band, a detailed  
<sup>214</sup> discussion on this is presented in [section 3.3](#).

### *3.2. Climatology of zooplankton biomass and standing stock*

Off Kanyakumari, z175 is shallower from May onward till October and the zooplankton biomass is comparatively higher than rest of the year (Fig. 5 g1). The D23 isotherm along-with oxycline (marked by  $2.1 \text{ ml L}^{-1}$ , a higher oxygen contour as it lies outside OMZ core) follows the same seasonal cycle like D175. However, there is almost no seasonal variation in ZSS off Kanyakumari ( $\sigma$ ,  $0.67 \text{ gm m}^{-2}$ ) as compared to the chl-a variation ( $\sigma$ ,  $1.53 \text{ mg m}^{-3}$ ). At the nearest northern mooring site off Kollam, a strong seasonal cycle is observed and the D215 is deeper for any given month. A decline (steep-rise) in ZSS (chl-a biomass) is seen and its minimum (peak) is attained in August (Fig. 5 f2). This feature was previously reported by A22, highlighting an imbalance in the interaction between zooplankton and phytoplankton, it occurs due to shallowing of thermocline and low oxygen, and that's why the ZSS is at its minimum when chl-a peaks. A similar feature is seen further north, off Udupi which sits at the transition zone of SEAS and CEAS, albeit with a relatively weaker zooplankton biomass and minimum (peak) of ZSS (chl-a) occurring a month later during September.

The D215 seasonal trend off Goa in present study is similar to trend of D215 off Goa as described in A22 (See section S1 for comparison). The biomass off Goa decreases rapidly below the z215 as reported earlier, reaching as low as  $60 \text{ mg m}^{-3}$  at 130 m during June to September (Fig. 5 d1). The ZSS off Jaigarh is identical but stronger to that of off Goa, owing to higher biomass above z215 and the comparatively deeper D215 (Fig. 5 c1). What's intriguing is a presence of strong variation in ZSS off Jaigarh ( $\sigma$ ,  $3.24 \text{ gm m}^{-2}$ ) highest among all locations although the seasonal variation in chl-a biomass (Fig. 5 c2) is visibly non-existent ( $\sigma$ ,  $0.05 \text{ mg m}^{-3}$ ) and lowest among all locations. This is an exact opposite scenario of Kanyakumari, where an insignificant seasonal variation in ZSS is seen even though the chl-a biomass

varies strongly. Starting from Kollam ([Fig. 5 f1](#)) and moving northward to Jaigarh  
250 ([Fig. 5 c1](#)), we see that the core of high zooplankton biomass gradually shifts from  
summer (off Kollam) to winter monsoon (off Jaigarh), with the transition of upper  
252 ocean zooplankton biomass happening along Udupi and Goa. On the contrary, chl-a  
biomass tends to have low seasonal range as we move northward from SEAS, with  
254 Jaigarh having the least seasonal variation. This shift along with winter monsoon  
facilitated deeper thermocline leads to an even larger impact on ZSS.

256 Further north off Mumbai the D215 is deeper in December to early April, re-  
sulting in a higher ZSS ([Fig. 5 b2](#)). D23 follows D215 and the oxycline follows an  
258 erratic pattern, reaching depths  $> 140$  m during January to March; when a higher  
biomass is observed above z215. The chl-a biomass shows seasonal variation albeit  
260 lower than the SEAS counterpart. At the northernmost site of EAS i.e, off Okha,  
biomass above z175 is much weaker leading to a relatively lower ZSS ([Fig. 5 a1, a2](#))  
262 compared to Mumbai. There's two chl-a peak off Okha, one in February due to con-  
vective mixing induced deepening of MLD ([Wiggert et al., 2005](#); [Lévy et al., 2007](#);  
264 [Shankar et al., 2016](#); [Keerthi et al., 2017](#)) and the other during August in summer  
monsoon ([Wiggert et al., 2005](#); [Lévy et al., 2007](#)). The ZSS remains flat during June  
266 to September, although the chl-a biomass increases in this time. Afterwards, ZSS  
gradually increases and attains its maximum in February same as the chl-a biomass.  
268 A comparison is drawn to the results of A22 in section S1.

### 3.3. Seasonal cycle and variability

270 This section will deal with a discussion on the seasonal cycle and variability of  
biomass and ZSS in annual and intra-annual scale along the three regimes of EAS.  
272 To understand the variation at a specific period, say 365-days (annual cycle) or 180-  
days (semi-annual cycle), wavelet analysis is carried out for biomass ([Fig. 6](#)) and

274 ZSS ([Fig. 7](#)). However, if we wish to understand the variation in a specific period band, we use Lanczos filtered time series. A brief discussion on the above mentioned  
276 techniques and variability in distinct period band is given in section S2.

278 From the linear equation correlating biomass and backscatter, the upper and lower bound of error limits equals to  $\sim 14 \text{ mg m}^{-3}$  ([Fig. 2](#)). The standard deviation of intra-annual (annual) variability is comparable to (less than) the error range of  
280 biomass vs backscatter relation. However, we are limited by the gaps in time series as discussed in [section 2.2.1](#). Therefore, we consider locations other than Okha and  
282 Jaigarh for the 40 m biomass and ZSS in annual scale.

284 The seasonal cycle is the sum total of annual, semi-annual cycle and their variabilty. The annual cycle of biomass off Kanyakumari (Udupi and Kollam) is weak  
286 (strong), but it varies in time ([Fig. 6](#)). For example off Kollam, the wavelet power is stronger post 2020. Wavelet analysis of the ZSS time series, derived from integrated  
288 biomass between 24 and 120 meters depth, indicates absence (presence) of annual cycle off Kanyakumari (off Udupi) ([Fig. 7 g1](#)). To capture the annual variability, the  
290 biomass is passed through Lanczos filter within period of 300 to 400 days ([Fig. 8](#)). The annual variability off Kanyakumari is least among all mooring sites. Kollam shows  
292 strong annual variability indicating prominent year-to-year variation of biomass. The intra-annual band ([Fig. 9](#)) tends to be stronger compared to the annual band. Much like the annual cycle, the semi-annual cycle is weak and intra-annual variability is  
294 moderate off Kanyakumari compared to Kollam and Udupi. However, the strong variability in intra-annual scale is restricted to upper ocean for few years off Kollam,  
296 where minor spectra around 120 days is also observed.

298 Off Goa, the annual cycle of biomass is comparatively weak contrary to the results of A22, possibly due to shorter time record and low biomass in the recent years as reflected in its ZSS wavelet for 2018 to early 2020 (2021 and 2022) ([Fig. 7](#)) resulting

300 in a weak (strong) annual variability ([Fig. 8](#)). Off Goa and Jaigarh, the semi-annual  
301 cycle tends to be strong, specifically during 2022 when a anomalous bloom is observed  
302 throughout EAS. The semi-annual cycle weakens with depth in these locations. Intra-  
303 annual component of seasonal cycle is observed off Goa, with weak (strong) variability  
304 during 2019 (2020, 2022) and is moderately strong off Jaigarh ([Fig. 9](#)). Energy is  
305 spread among all intra-annual periods for 2022 off Goa ([Figs. 6](#) and [7](#)), while during  
306 2019 and 2020 the wavelet energy is only present in the semi-annual periods resulting  
307 in a overall weaker intra-annual component ([Fig. 6](#)).

308 Further north, a strong annual cycle is seen off Mumbai with strong annual vari-  
309 ability highest among EAS sites ([Fig. 8](#)). Biomass variability in annual scale de-  
310 creases minutely with depth off Mumbai and the three CEAS sites than off Kollam  
311 ([Fig. 8](#)) similar to the observed ocean currents ([Chaudhuri et al., 2020, 2021](#)). The  
312 annual cycle and annual variability of biomass and subsequently, ZSS increases along  
313 the slope as we go northward to Mumbai from Kanyakumari. The intra-annual band's  
314 strength is reduced off Mumbai and Okha as compared to CEAS and SEAS, and the  
315 intra-annual variability also decreases more with depth as we go equatorward. The  
316 semi-annual cycle is moderately present at 40 m off Mumbai which weakens at 104  
317 m resulting in higher contribution of annual cycle to ZSS. Analysis reveals the pres-  
318 ence of moderately strong semi-annual cycle off Okha but only at 104 m and it's  
319 intra-annual (annual) band is similar (weaker) in magnitude as compared to Mum-  
320 bai. Excluding Kanyakumari, intra-annual variability of biomass decreases poleward  
321 with higher variation seen off Kollam and Udupi similar to the WICC ([Amol et al.,](#)  
322 [2014; Chaudhuri et al., 2020](#)).

#### 4. Interannual variability

324 Aberrations from the seasonal cycle occurs due to the variations in interannual  
and intraseasonal scales, we deal with the former (later) in this (next) section. The  
326 presence of interannual variability in zooplankton biomass is not well observed or  
understood previously due to lack of continuous long-term data. Unlike previous  
328 studies ([Madhupratap et al., 1996a; Jyothibabu et al., 2010](#)), the work carried out  
using long continuous time series by A22 was able to shed light on the seasonal cycle  
330 and hinted on the strong interannual variability at Kollam, a feature that was not  
seen at rest of the sites. We've used the latest ADCP records along with data used in  
332 A22 off Mumbai, Goa, and Kollam to show strong presence of interannual variability.

From the biomass time series off Kollam, a higher biomass is observed for the  
334 years 2016, 2018–2019, and 2022–2023 ([Fig. 3](#)) with deeper D215. It is low for the  
years 2013 and to a great extent during 2020 and the D215 is shallow enough to touch  
336 depths up to  $\sim$ 20 m and above throughout the year. This reason led us to discard  
D215 for 2020 in our analysis. Multi-year long high or low biomass is coming from  
338 its underlying interannual variability ([Figure S2](#)). As seen in the monthly resampled  
biomass time series off Kollam, the magnitude of interannual component is higher  
340 than the annual variability, and it masks the underlying weaker annual component  
irrespective of whether it is strongly positive or negative. The wavelet spectra of  
342 daily biomass at 40 m is able to register the quasi-biennial oscillations ( $\sim$ 720 days)  
observed in this time series. Off Goa however, the biomass doesn't show much year-  
344 to-year variations resulting in lack of spectra within the Cone of Influence (CoI),  
but the spectra shows up at seasonal and intraseasonal scales and also in biennial  
346 period though it lies beyond CoI from 2020 onward. Further north, Mumbai have  
the strongest observed annual cycle as discussed using recent data ([Fig. 6](#)), but the

<sup>348</sup> appended data from A22 shows evidence of variability at  $\sim$ 720 days (Figure S2).  
<sup>350</sup> The variability off Kanyakumari as inferred from it's biomass time series is similar  
<sup>352</sup> to that of off Kollam, such as during 2020 when both the sites had low biomass year  
round, but since the mean biomass at any given depth above its z175 is lower than  
the z215 off Kollam, the impact of interannual variability is reflected prominently at  
the later site.

<sup>354</sup> **5. Intraseasonal variability**

<sup>356</sup> On the similar lines as discussed in the preceding section, intraseasonal variabil-  
<sup>358</sup> ity of biomass is defined as shifts occurring within a season, typically lasting few  
days to few weeks and is driven by short-term environmental changes, e.g., nutri-  
<sup>360</sup> ent replenishment (depletion) in short-span due to upwelling and/or entrainment  
(bloom). The variability can be split into two categories; a high-frequency (period  
<sup>362</sup>  $<$  30 days) and a low-frequency ( $30 <$  period  $<$  90 days) component. The presence  
of significant variation in the 30-day running mean with recurring bursts are seen  
<sup>364</sup> in the daily data and in the wavelet analysis of biomass at 40 and 104 m ([Fig. 6](#))  
lasting few days to a week and distinctive to each location. Most of the spikes in  
<sup>366</sup> biomass are occurring due to the high-frequency component of intraseasonal band,  
but our focus is on the low-frequency component seen as bursts lasting much longer  
<sup>368</sup> than biomass spikes. Much like the intra-annual variability, the standard deviation  
of intraseasonal component is comparable or higher than the error range of unfiltered  
biomass vs backscatter relation.

<sup>370</sup> The strength and contribution of variability components changes over time and  
differs between EAS regimes as discussed in [section 3.3](#). From the wavelet analysis  
of biomass at 40 and 104 m, peaks in low-frequency intraseasonal band is observed  
<sup>372</sup> across EAS. But the variability can be different at upper and lower regimes at a

given location within a specific period band. This difference is evident e.g., during  
374 2019–2021 off Kanyakumari, the wavelet power of biomass within the intraseasonal  
band declines as we go deeper from 40 m ([Fig. 6](#)). The filtered biomass in intrasea-  
376 sonal band also showcases the decrease in variability with respect to depth for the  
same period off Kanyakumari ([Fig. 10](#)). This holds true across EAS with the excep-  
378 tion of very few years where the variability at 104 m is comparable or higher than  
biomass variability at surface layers. However, in other few instances, such as during  
380 September–November of 2018 off CEAS, intraseasonal variability remains consistent  
throughout the entire water column.

382 Strong intraseasonal variability off Kanyakumari relative to the variability in  
its annual band, along-with comparable or lower range of intra-annual variability  
384 ([Fig. 11](#)) and the wavelet at 40 and 104 m indicates that the short-lived environ-  
mental changes is a major driver of its biomass alongside minor seasonal variation.  
386 Off Kollam and Udupi, the presence of intraseasonal bursts is prominent, but due  
to an equal strength of intra-annual component the biomass isn't solely driven by  
388 short-term environmental changes. For instance, in 2019 off Kollam ([Fig. 11](#)), low  
frequency intraseasonal variability was weak during summer monsoon but an increase  
390 in biomass during the same period was due to an increase intra-annual component.  
However, a sharp decline in August 2019 resulted from reduced intra-annual and  
392 intraseasonal variability, even with the presence of a weakly positive annual variability.

Off Goa, strong peaks in intraseasonal band is present in wavelet spectra of  
394 biomass. During early 2019 to late 2020, the intra-annual variability off Goa is non-  
existent and with the weak annual variability ([Fig. 11](#)), a rather seasonally invariant  
396 biomass at 40 and 104 m is observed but the presence of intraseasonal variations  
is seen at both 40 and 104 m ([Fig. 4](#)). The wavelet peaks in intraseasonal band  
398 occurred strongly in 2018 and later in 2020, but the absence intra-annual band in

2019 makes it easier to comprehend the contribution of intraseasonal variability. A  
400 similar feature is noted off Jaigarh albeit with a weaker magnitude. Weak presence  
of intraseasonal variability is noticed in the relatively smoother 30-day rolling mean  
402 biomass off Mumbai and Okha. During early 2021 off Mumbai, the presence of  
strong intraseasonal peaks in wavelet spectra of 104 m along with 40 m ([Fig. 6](#))  
404 shows up in biomass variability in intraseasonal scale ([Fig. 10](#)). Although spectra in  
the intraseasonal band is present at 40 m off Mumbai and Okha, it is almost absent  
406 at 104 m except for a select few years. It implies that at some locations the strong  
variability may occur at deeper depth even when the upper ocean is showing lower  
408 variability. Off Okha, the intraseasonal variability is lowest among all EAS sites  
followed by Mumbai. However, Okha has weak annual and intra-annual variability  
410 unlike Mumbai leading to least predictability.

The biomass variability at 40 and 104 m in intraseasonal scale is well reflected  
412 in the ZSS time series and the corresponding wavelet spectra ([Fig. 7](#)). While 40 m  
biomass varies strongly Off SEAS, the biomass variation at 104 m is weaker in com-  
414 parison leading to upper ocean determined ZSS. There are instances when both 40  
and 104 m biomass are in phase leading to a stronger ZSS variation e.g., September–  
416 November 2019 off Kanyakumari ([Figure S3](#)) though biomass variation at 104 m is  
weak ([Fig. 10](#)). At instances such as during June–July 2018 and Mar–July 2019 at  
418 the above location, when the 40 and 104 m biomass are anti-phase or not in phase,  
they result in a reduced ZSS ([Figure S3](#)). No annual and semi-annual cycle seems  
420 to be present in ZSS off Kanyakumari, but presence of bursts lasting few days to  
weeks are an indication of intraseasonal variations. While off Kollam and Udupi, the  
422 presence of strong intra-annual variations is observed in ZSS alongside intraseasonal  
variation dominant during September–November. Off Goa and Jaigarh during early  
424 2019 to late 2020, the intra-annual and annual variations are much weak but strong

intraseasonal variation leads to bursts in biomass. The resulting ZSS at these locations shows strong intraseasonal bursts but seasonal variation is weaker (([Fig. 7](#)) d2, c2). Strength of intraseasonal variability in biomass is reduced at NEAS ([Fig. 10](#)) leading to a comparatively smoother ZSS in 30-day rolling mean data ([Fig. 7](#) a2, b2).

The intraseasonal peaks in biomass and further ZSS are strong in SEAS followed by CEAS and is weak off NEAS sites ([Fig. 10](#)). Variability in intraseasonal scale seems to occur predominantly during August to November, for example off Kanyakumari (2018, 2019 and 2020), off Kollam (2018, 2021 and 2022) and off Udupi (2018) although it can extend to mid-summer/mid-winter monsoon for few years and is coherent along much of the EAS slope as seen during 2018 at intraseasonal band or sometimes even at scale of few days ([Fig. 11](#)). Coherence and strong variability at deeper depths at instance (during early 2021 off Mumbai) indicates possible role of ocean circulation in determining biomass at intraseasonal periods. Also, the magnitude of intraseasonal variability of 40 m (104 m) biomass decreases (increases) as we move poleward ([Fig. 11](#)), the 40 m variance is much like the observed intraseasonal currents ([Amol et al., 2014; Chaudhuri et al., 2020, 2021](#)). However, the strength of intraseasonal variability of biomass is in contrast to the corresponding band of WICC which is strong during winter monsoon along the slope ([Amol et al., 2014; Chaudhuri et al., 2020](#)) and shelf ([Chaudhuri et al., 2021](#)) suggesting further study to identify any possible connection. Nonetheless, the backscatter derived biomass in higher sampling frequency is essential for discussing the intraseasonal variability, whereas conventional sampling method such as with research vessel, where one snapshot of biomass is taken in an interval of 15–30 days, would fail to capture these bursts in biomass.

## 6. Discussion

### 450 6.1. Summary

The zooplankton biomass and standing stock across different regions of EAS was  
452 examined in this article, highlighting their spatio-temporal trends in the light of  
physico-chemical parameters using the multi-yearlong ADCP backscatter data from  
454 2017 to 2023.

The findings shows notable seasonal variation in zooplankton biomass and ZSS;  
456 in SEAS the higher biomass is observed during summer monsoon, while in NEAS  
the high biomass is observed during winter monsoon with transition of peak biomass  
458 happening gradually along CEAS ([section 3.2](#)). Off Kollam, a unique double peak  
in ZSS occurs, one during May to July and another in September to November, sug-  
460 gesting a complex interplay between environmental drivers and zooplankton growth  
([Fig. 5 f2](#)). Off Kanyakumari, the seasonal variation in ZSS is non-existent even  
462 though a dramatic seasonality is seen in chl-a. On contrary, Jaigarh shows strong  
variation in ZSS where the chl-a variation is non-existent. Such feature was observed  
464 at embayment west off Antarctic peninsula and has been attributed to advective  
influx ([Espinasse et al., 2012](#)) but the distinct dynamics of EAS and Antarctica im-  
466 plies the causality may not be same. Climatology shows strong decline in biomass  
w.r.t. depth off Goa, then NEAS sites off Jaigarh, Mumbai and Okha followed by  
468 SEAS locations off Udupi, Kollam and Kanyakumari. The minor peak observed off  
Mumbai in A22's climatology is absent in the climatology presented using the recent  
470 data.

Seasonal cycle and variability play a crucial role in regulating biomass. A strong  
472 annual cycle is observed at NEAS ([Fig. 6](#)), with biomass peaking during winter  
monsoon months ([Fig. 5](#)) and deeper D215, the annual cycle weakens as we got

equatorward. CEAS and SEAS regions particularly off Kollam, exhibit more complex patterns. Off Kollam, the presence of a weak annual cycle and a stronger semi-annual cycle is noted along with a strong quasi-biennial cycle agreeing with A22. The semi-annual cycle is especially prominent in the SEAS ([section 3.3](#)), where it contributes significantly to the seasonal biomass changes. The variability in annual scale is weak, while that in intra-annual scale is often comparable to intraseasonal variability which is found to influence zooplankton biomass strongly in the summer to winter monsoon transition months ([Fig. 10](#)). The high (low) frequency component of intraseasonal variability determine changes lasting for days (few days to weeks) observed as spikes (bursts) in the daily biomass record ([Fig. 11](#)). Intraseasonal variability is higher in the SEAS, with the NEAS displaying less variance. The intraseasonal variability is often restricted to the upper layer, and it is expected owing to higher variability of chl-a at surface which weakens with increasing depth. The affect of intraseasonal variability compounded with presence of strong intra-annual is observed in the difference of mean biomass at 40 and 104 m ([Fig. 4](#)). The intraseasonal variations may exist throughout the water column for few years and can be coherent along the slope possibly suggesting that the penetration and propagation of currents in intraseasonal band ([Amol et al., 2012, 2014; Chaudhuri et al., 2020](#)) could be driving biomass on few occasions. The reduction/enhancement of ZSS on account of out-of-phase/in-phase upper and lower depth biomass occurs at annual and intra-annual and intraseasonal time scales ([Figure S3](#)).

## *6.2. consequences of intraseasonal variability*

It is evident that the intraseasonal variability dominates the zooplankton biomass along EAS regime ([section 5](#)). A strong intraseasonal component suggests implications on sampling, zooplankton patchiness and its predictability.

### 6.2.1. Implication on sampling

500      Zooplankton biomass exhibits significant intraseasonal variability driven by dynamic oceanographic processes which operate over short temporal scales and vary in space ([section 5](#)). Since the strength of intraseasonal component is higher than the other two variabilities ([Fig. 11](#)) and its high-frequency component is rather erratic, dependency of zooplankton biomass on the intra-seasonal variation has implication 504 on the sampling of zooplankton using cruises. A servicing cruise along the EAS moorings takes about 12 to 15 days excluding the time to and fro from port to first/last 506 mooring ([Chaudhuri et al., 2020](#); [Aparna et al., 2022](#)). However, a sampling cruise 508 dedicated to study the spatial variation of zooplankton ([Madhupratap et al., 1992](#); [Smith et al., 1998](#); [Wishner et al., 1998](#); [Kidwai and Amjad, 2000](#)), say for summer 510 monsoon may last a month or more with coarse sampling interval and hence fail to capture the actual biomass within a season for a fair spatial comparison.

512      Consider the cruise undertaken to address the seasonality in zooplankton abundances and composition ([Madhupratap et al., 1996a](#)) in Arabian Sea as part of 514 JGOFS program. The first, second and third cruises of this study was taken 12 April to 12 May 1994 (inter-monsoon), 3 February to 4 March 1995 (winter) and 20 July to 12 August 1995 (summer), respectively. It is imperative to acknowledge that 516 sampling done twice (once in mid-day and again in mid-night), and two snapshots are held as a representative of the entire season. Does this sampling method give accurate idea about the zooplankton biomass in a particular season? The comparison 518 of variability in intraseasonal periods is used to shed a light on the biomass variation within a season. Consider the summer monsoon months, off Mumbai during early 520 June of 2019 ([Fig. 11](#)), where a spike in biomass is observed due to an instantaneous increase in the high-frequency component of biomass variability resulting in an in-

crease of  $\sim 150 \text{ mg m}^{-3}$  within few days. Similar spikes are seen at other locations too, e.g., off Kollam during July end and multiple instances in September of 2019 (Fig. 11). These spikes lasts only for a day to few days but the bursts in biomass tend to last longer from a few days to a few weeks. A burst is seen in biomass during September 2019 off Kanyakumari, but the preceding summer monsoon months had an almost invariant biomass with minor bursts, both of which won't be captured by a conventional ship based sampling. Second limitation of cruise based sampling is spatial constraint. For the same year 2019 off Kanyakumari, the burst in biomass during September is followed by a decline during October which results in a biomass difference of about  $\sim 160 \text{ mg m}^{-3}$  within a month and most of it is contribution from intraseasonal variability (Fig. 11). This burst is also observed off Kollam, Udupi till Goa, albeit with decreasing intensity as we go poleward. Such coherency can only be observed if continuous and frequent measurements were taken across EAS. The spatial map of mesozooplankton distribution such as one by Jyothibabu et al. (2010) for each season (see Fig. 11 of Jyothibabu et al. (2010)) is limited by sampling frequency and time elapsed to cover stations, and the measured biomass is prone to distortion since biomass is subject to drastic changes within few days. The limitations of cruise based sampling leads to inaccurate depiction of biomass in space and time, and it can be mitigated by usage of ADCP backscatter derived zooplankton biomass.

#### 6.2.2. Zooplankton patchiness

Poor sampling coverage and intermittent measurement also impacts assessment of zooplankton patchiness, defined as the aggregations arising in response to temperature, salinity and oxygen gradients, currents, variation in light intensity, predator-prey concentrations (Folt and Burns, 1999; Raghukumar and Anil, 2003). Though the usage of traditional sampling methods has led to determination of zooplankton

abundance and distribution in EAS (Madhupratap et al., 1992, 1996a; Khandagale  
550 et al., 2022), the biomass measurements can miss or rarely sample the patches of  
zooplankton, and thereby misinterpret abundance by under/over-estimation of the  
552 standing stock. A high intraseasonal variability in zooplankton biomass suggests that  
patchiness in the deep-sea environment occurs within individual seasons on periods  
554 equivalent to few days to few weeks. During July 20–31st 2019, a spike lasting few  
days in daily biomass at 40 m (Fig. 11) is observed at most of the EAS sites, albeit  
556 with differing magnitude followed by a sharp decline and difference in occurrence of  
maximum biomass by few days. But the coherence doesn't exist at all instances .  
558 For example, during 13th June 2019, the instantaneous spike in biomass observed  
off Mumbai is not seen anywhere else, but the low biomass lasting about 2 weeks in  
560 dates adjacent to this spike is seen at Okha, Mumbai, Jaigarh and Goa (Fig. 11).  
The observed spikes in zooplankton biomass, as discussed in the preceding subsec-  
562 tion, occurring within just a few days, are a clear example of the zooplankton cluster  
formation. The patchiness can also exist on longer periods. During 15 January–15  
564 February 2019, a burst is observed off Udupi lasting about 20–30 days, while it is  
missing at its nearby moorings, signifying presence of patchiness and its prominence  
566 in the longer periods of intraseasonal band. However, there are occasions such as  
during September–November 2018 (Fig. 10) and 2019 (Fig. 11) when the coherence  
568 in biomass is observed indicating plausible collapse of patchiness.

The zooplankton patchiness occurring in longer periods of intraseasonal band is  
570 likely associated with processes such as fronts (Coyle and Hunt, 2000; Wade and  
Heywood, 2001; Hitchcock et al., 2002), pulsed inputs of nutrients in open ocean  
572 water (Anil et al., 2021) and biological processes (Folt and Burns, 1999), while those  
occurring in shorter periods could be due to physical convergence (Napp et al., 1996)  
574 of zooplankton. The higher variance in deeper layers off Okha could be an indication

of deep-living zooplankton species (Raghukumar and Anil, 2003) due to strong oxygen gradient. Thus, a lack of feasibility in intensive in-situ sampling suggests that the data collected might not be representative of the actual standing stock being studied (Smith et al., 1998) and may not capture zooplankton patches.

#### 6.2.3. Predictability

Though EAS shows a strong seasonal cycle of current, there are notable differences between regimes of EAS. Kollam's seasonal cycle is marked by intense intraseasonal bursts making the shelf WICC at Kollam highly unpredictable (Chaudhuri et al., 2021) and the intraseasonal variability increases equatorward. The direction of WICC at any given time of the year can be either poleward or equatorward owing to the bursts. Similarly, the zooplankton biomass varies frequently and strongly within the season itself (section 5) across EAS. From the preceding subsection, it is inferred that though not often, coherence is observed in both the lower and higher periods of intraseasonal band leading to collapse of patchiness. The presence of coherence implicates better predictability of biomass especially during September–November as observed during 2018 and 2019. However, rest of the time in absence of coherence in few months, patchiness takes over and the zooplankton biomass is erratic with sudden spikes and lasting bursts. This indicates that zooplankton form and patches fluctuate due to short-term changes, possibly responding to ocean environment (Folt and Burns, 1999; Raghukumar and Anil, 2003; Anil et al., 2021). Hence, the zooplankton biomass much like the current is dominated by intraseasonal variations more than the annual cycle indicating possible loss in predictability.

Understanding the currents and phytoplankton variability and their relation to zooplankton would enable us to have better predictability. The occurrence of strong biomass intraseasonal variability before winter monsoon, the similarity in trend of

600 increasing (decreasing) intraseasonal and intra-annual (annual) variability of biomass  
601 and currents as we go equatorward along the EAS slope, presence strong interannual  
602 variability in biomass and currents and quasi-biennial cycle that is associated with  
603 Indian summer-monsoon rainfall ([Mooley and Parthasarathy, 1984](#); [Bhalme et al., 1987](#);  
604 [Meehl and Arblaster, 2002](#)), all these are tempting as it indicates a link between  
605 the two. However, a rigorous study is necessary to excavate any such relationship.  
606 Strong peaks in intraseasonal band in chl-a was evident in Lomb–Scargle periodogram  
607 (Figure S4), analogous to zooplankton biomass and ZSS, but lacked concrete evidence  
608 of direct correlation.

### 6.3. Conclusion

610 The results presented in this paper are based on the ADCP backscatter which  
611 is suitable for creating long-term time series of zooplankton biomass in open ocean  
612 ([Jiang et al., 2007](#); [Hobbs et al., 2021](#); [Ursella et al., 2021](#); [Aparna et al., 2022](#)). There  
613 are however, certain limitations to this approach of studying biomass using ADCP  
614 backscatter as proxy. While the variation in depth is captured with in-situ samples  
615 from MPN, the variation in season is not adequately addressed owing to the limitation  
616 of months when ADCP servicing cruises are undertaken apart from availability. The  
617 west coast cruises for ADCP servicing are planned for the monsoon transition months  
618 but may start as early as late September till December with few exceptions such as  
619 2022 when it was carried out in March. Since the intraseasonal and intra-annual  
620 variability is almost double that of the annual one ([section 5](#)), the sampling done  
621 in particular season for biomass-backscatter comparison isn't sufficient but can be  
622 mitigated with extensive season-wise sampling ([Jadhav and Smitha, 2024](#)), however  
623 in their study, the difference in biomass between seasons was about  $15 \text{ mg m}^{-3}$   
624 which is comparable to error bar associated with our backscatter-biomass linear

regressed equation. The second limitation is lack of any information regarding the  
626 size distribution of zooplankton and their contribution to ZSS is lost.

The merits outshine above mentioned disadvantages in the unique aspect that  
628 a sufficiently long and continuous time series of zooplankton biomass could be con-  
structed upon which further analysis can be carried out. Along-with the discussion  
630 on seasonal and further the climatological cycle, we provided evidence of strong  
intraseasonal variation; this has three major implications: 1) on the conventional  
632 sampling methods used to assess the zooplankton biomass and standing stock, and  
the snapshots provided by such samples aren't representative of a season; 2) on the  
634 zooplankton patchiness, and further on the under or over estimation of standing  
stock; 3) on the predictability which is reduced due to strong biomass variation at  
636 intraseasonal scale, and the presence of patchiness as spikes and bursts. The possible  
influence of ocean currents could be explored using the current data from ADCPs  
638 ([Hitchcock et al., 2002](#); [Lawson et al., 2004](#)). It is evident that a mono-frequency  
ADCP is adequately suitable to capture the intraseasonal variations of zooplankton  
640 biomass that will otherwise be left inaccessible by traditional methods.

## 7. Declaration of competing interest

642 The authors declare that they have no known competing financial interests or  
personal relationships that could have appeared to influence the work reported in  
644 this paper.

## 8. Acknowledgments

646 The present work has been funded by CSIR (Council of Scientific and Indus-  
trial Research, New Delhi, India) and INCOIS (Indian National Centre for Ocean

648 Information Services, Hyderabad, India) under the COSINE (Current Observations  
and Simulations in the Indian EEZ) project as part of OSMART Programme. Sup-  
650 port of the mooring division and ship cell of CSIR-NIO is acknowledged for their  
contribution. Ranjan Kumar Sahu expresses his acknowledgment to the Council of  
652 Scientific and Industrial Research (CSIR) for sponsoring his fellowship. Additionally,  
he extends his thanks to Mr. Ashok Kankonkar for providing the essential data, Mr.  
654 Rahul Khedekar for his help in processing backscatter data, Mr. Roshan D'Souza for  
his contribution in processing of zooplankton data. Their contributions were invaluable  
656 to the successful completion of our research. This is NIO contribution number  
XXXX.

658 **References**

- 660 Almén, A.K., Tamelander, T., 2020. Temperature-related timing of the spring bloom and match  
between phytoplankton and zooplankton. Mar. Biol. Res. 16, 674–682. doi:<https://doi.org/10.1080/17451000.2020.1846201>.
- 662 Amol, P., Bemal, S., Shankar, D., Jain, V., Thushara, V., Vijith, V., Vinayachandran, P.N., 2020.  
Modulation of chlorophyll concentration by downwelling rossby waves during the winter monsoon  
664 in the southeastern arabian sea. Prog. Oceanogr. 186, 102365. doi:<https://doi.org/10.1016/j.pocean.2020.102365>.
- 666 Amol, P., Shankar, D., Aparna, S.G., Shenoi, S.S.C., Fernando, V., Shetye, S.R., Mukherjee, A.,  
Agarvadekar, Y., Khalap, S., Satelkar, N.P., 2012. Observational evidence from direct current  
668 measurements for propagation of remotely forced waves on the shelf off the west coast of india.  
J. Geophys. Res. Oceans 117. doi:<https://doi.org/10.1029/2011JC007606>.
- 670 Amol, P., Shankar, D., Fernando, V., Mukherjee, A., Aparna, S.G., Fernandes, R., Michael,  
G.S., Khalap, S.T., Satelkar, N.P., Agarvadekar, Y., Gaonkar, M.G., Tari, A.P., Kankonkar,  
672 A., Vernekar, S., 2014. Observed intraseasonal and seasonal variability of the west india  
coastal current on the continental slope. J. Earth Syst. Sci. 123, 1045–1074. doi:<https://doi.org/10.1007/s12040-014-0449-5>.
- 676 Anil, A.C., Desai, D.V., Khandeparker, L., Krishnamurthy, V., Mapari, K., Mitbavkar, S., Patil,  
J.S., Sarma, V.V.S.S., Sawant, S.S., 2021. Short term response of plankton community to  
nutrient enrichment in central eastern arabian sea: Elucidation through mesocosm experiments.  
678 J. Environ. Manage. 288, 112390. doi:<https://doi.org/10.1016/j.jenvman.2021.112390>.

- 680 Aparna, S.G., Desai, D.V., Shankar, D., Anil, A.C., Dora, S., Khedekar, R.R., 2022. Seasonal  
cycle of zooplankton standing stock inferred from adcp backscatter measurements in the eastern  
arabian sea. *Prog. Oceanogr.* 203, 102766. doi:<https://doi.org/10.1016/j.pocean.2022.102766>.
- 684 Banse, K., 1968. Hydrography of the arabian sea shelf of india and pakistan and effects on demersal  
fishes, in: Deep Sea Res. Oceanogr. Abstr., Elsevier. pp. 45–79. doi:[https://doi.org/10.1016/0011-7471\(68\)90028-4](https://doi.org/10.1016/0011-7471(68)90028-4).
- 686 Banse, K., 1995. Zooplankton: pivotal role in the control of ocean production: I. biomass and  
production. *ICES J. Mar. Sci.* 52, 265–277. doi:[https://doi.org/10.1016/1054-3139\(95\)80043-3](https://doi.org/10.1016/1054-3139(95)80043-3).
- 690 688 Banse, K., English, D.C., 2000. Geographical differences in seasonality of czcs-derived phytoplank-  
ton pigment in the arabian sea for 1978–1986. *Deep Sea Res. Part II Top. Stud. Oceanogr.* 47,  
1623–1677. doi:[https://doi.org/10.1016/S0967-0645\(99\)00157-5](https://doi.org/10.1016/S0967-0645(99)00157-5).
- 692 Barber, R.T., Marra, J., Bidigare, R.C., Codispoti, L.A., Halpern, D., Johnson, Z., Latasa, M.,  
694 Goericke, R., Smith, S.L., 2001. Primary productivity and its regulation in the arabian sea  
during 1995. *Deep Sea Res. Part 2 Top. Stud. Oceanogr.* 48, 1127–1172. doi:[https://doi.org/10.1016/S0967-0645\(00\)00134-X](https://doi.org/10.1016/S0967-0645(00)00134-X).
- 696 Batchelder, H.P., VanKeuren, J.R., Vaillancourt, R.D., Swift, E., 1995. Spatial and temporal  
distributions of acoustically estimated zooplankton biomass near the marine light-mixed layers  
698 station ( $59^{\circ}30'N$ ,  $21^{\circ}00'W$ ) in the north atlantic in may 1991. *J. Geophys. Res. Oceans* 100,  
6549–6563. doi:[10.1029/94jc00981](https://doi.org/10.1029/94jc00981).
- 700 Bemal, S., Anil, A.C., Shankar, D., Remya, R., Roy, R., 2018. Picophytoplankton variability:  
Influence of winter convective mixing and advection in the northeastern arabian sea. *J. Mar.  
702 Syst.* 180, 37–48. doi:<https://doi.org/10.1029/2001GL013422>.
- 704 Bhalme, H.N., Rahalkar, S.S., Sikder, A.B., 1987. Tropical quasi-biennial oscillation of the 10-  
mb wind and indian monsoon rainfall-implications for forecasting. *J. Climatol.* 7, 345–353.  
doi:<https://doi.org/10.1002/joc.3370070403>.
- 706 Brock, J.C., McClain, C.R., 1992. Interannual variability in phytoplankton blooms observed in the  
northwestern arabian sea during the southwest monsoon. *J. Geophys. Res. Oceans* 97, 733–750.  
708 doi:<https://doi.org/10.1029/91JC02225>.
- 710 Brock, J.C., McClain, C.R., Luther, M.E., Hay, W.W., 1991. The phytoplankton bloom in the  
northwestern arabian sea during the southwest monsoon of 1979. *J. Geophys. Res. Oceans* 96,  
20623–20642. doi:<https://doi.org/10.1029/91JC01711>.
- 712 Chatterjee, A., Shankar, D., Shenoi, S.S.C., Reddy, G., Michael, G.S., Ravichandran, M., Gopalkrishna,  
714 V., Rama Rao, E., Udaya Bhaskar, T., Sanjeevan, V., 2012. A new atlas of temperature  
and salinity for the north indian ocean. *J. Earth Syst. Sci.* 121, 559–593. doi:<https://doi.org/10.1007/s12040-012-0191-9>.

- 716 Chaudhuri, A., Amol, P., Shankar, D., Mukhopadhyay, S., Aparna, S.G., Fernando, V., Kankonkar,  
A., 2021. Observed variability of the west india coastal current on the continental shelf from  
718 2010–2017. *J. Earth Syst. Sci.* 130, 1–21. doi:<https://doi.org/10.1007/s12040-021-01603-4>.
- 720 Chaudhuri, A., Shankar, D., Aparna, S.G., Amol, P., Fernando, V., Kankonkar, A., Michael, G.S.,  
Satelkar, N.P., Khalap, S.T., Tari, A.P., Gaonkar, M.G., Ghatkar, S., Khedekar, R.R., 2020.  
Observed variability of the west india coastal current on the continental slope from 2009–2018.  
722 *J. Earth Syst. Sci.* 129, 57. doi:<https://doi.org/10.1007/s12040-019-1322-3>.
- 724 Cisewski, B., Strass, V.H., Rhein, M., Krägesky, S., 2010. Seasonal variation of diel vertical  
migration of zooplankton from adcp backscatter time series data in the lazarev sea, antarctica.  
Deep Sea Res. Part I Oceanogr. Res. Pap. 57, 78–94. doi:<https://doi.org/10.1016/j.dsr.2009.10.005>.
- 728 Coyle, K.O., Hunt, G.L., 2000. Seasonal differences in the distribution, density and scale of zooplankton patches in the upper mixed layer near the western aleutian islands. *Plankton Biol. Ecol* 47, 31–42. URL: [https://www.plankton.jp/PBE/issue/vol47\\_1/vol47\\_1\\_031.pdf](https://www.plankton.jp/PBE/issue/vol47_1/vol47_1_031.pdf).
- 730 Deines, K.L., 1999. Backscatter estimation using broadband acoustic doppler current profilers, in: Proceedings of the IEEE Sixth Working Conference on Current Measurement (Cat. No. 99CH36331), IEEE. pp. 249–253. doi:<https://doi.org/10.1109/CCM.1999.755249>.
- 734 DeSousa, S.N., Dileepkumar, M., Sardessai, S., Sarma, V.V.S.S., Shirodkar, P.V., 1996. Seasonal variability in oxygen and nutrients in the central and eastern arabian sea, Indian Academy of Sciences. doi:<http://drs.nio.org/drs/handle/2264/35>.
- 736 Edvardsen, A., Slagstad, D., Tande, K.S., Jaccard, P., 2003. Assessing zooplankton advection in the barents sea using underway measurements and modelling. *Fish. Oceanogr.* 12, 61–74. doi:<https://doi.org/10.1046/j.1365-2419.2003.00219.x>.
- 740 Espinasse, B., Zhou, M., Zhu, Y., Hazen, E.L., Friedlaender, A.S., Nowacek, D.P., Chu, D., Carlotti, F., 2012. Austral fall- winter transition of mesozooplankton assemblages and krill aggregations in an embayment west of the antarctic peninsula. *Mar. Ecol. Prog. Ser.* 452, 63–80. doi:<https://doi.org/10.3354/meps09626>.
- 744 Flagg, C.N., Smith, S.L., 1989. On the use of the acoustic doppler current profiler to measure zooplankton abundance. *Deep Sea Res. Part A. Oceanogr. Res. Pap.* 36, 455–474. doi:[https://doi.org/10.1016/0198-0149\(89\)90047-2](https://doi.org/10.1016/0198-0149(89)90047-2).
- 746 Folt, C.L., Burns, C.W., 1999. Biological drivers of zooplankton patchiness. *Trends Ecol. Evol.* 14, 300–305. doi:[https://doi.org/10.1016/S0169-5347\(99\)01616-X](https://doi.org/10.1016/S0169-5347(99)01616-X).
- 748 García, H.E., Locarnini, R.A., Boyer, T.P., Antonov, J.I., Mishonov, A.V., Baranova, O.K., Zweng, M.M., Reagan, J.R., Johnson, D.R., 2014. Dissolved oxygen, apparent oxygen utilization, and oxygen saturation. NOAA Atlas NESDIS 75 3. URL: [https://data.noaa.gov/woa/WOA18/DOC/woa18\\_vol3.pdf](https://data.noaa.gov/woa/WOA18/DOC/woa18_vol3.pdf).

- 752 Greene, C.H., Wiebe, P.H., Pelkie, C., Benfield, M.C., Popp, J.M., 1998. Three-dimensional acoustic  
754 visualization of zooplankton patchiness. Deep Sea Res. Part II Top. Stud. Oceanogr. 45, 1201–  
1217. doi:[https://doi.org/10.1016/S0967-0645\(98\)00034-4](https://doi.org/10.1016/S0967-0645(98)00034-4).
- 756 Greenlaw, C.F., 1979. Acoustical estimation of zooplankton populations 1. Limnol. Oceanogr. 24,  
226–242. doi:<https://doi.org/10.4319/lo.1979.24.2.0226>.
- 758 Guerra, D., Schroeder, K., Borghini, M., Camatti, E., Pansera, M., Schroeder, A., Sparnocchia, S.,  
760 Chiggiato, J., 2019. Zooplankton diel vertical migration in the corsica channel (north-western  
mediterranean sea) detected by a moored acoustic doppler current profiler. Ocean Sci. 15, 631–  
649. doi:<https://doi.org/10.5194/os-15-631-2019>.
- 762 Hamilton, J.M., Collins, K., Prinsenberg, S.J., 2013. Links between ocean properties, ice cover, and  
plankton dynamics on interannual time scales in the canadian arctic archipelago. J. Geophys.  
Res. Oceans 118, 5625–5639. doi:<https://doi.org/10.1002/jgrc.20382>.
- 764 Hays, G.C., 2003. A review of the adaptive significance and ecosystem consequences of zooplankton  
diel vertical migrations, in: Migrations and Dispersal of Marine Organisms: Proceedings of the 37  
766 th European Marine Biology Symposium held in Reykjavík, Iceland, 5–9 August 2002, Springer.  
pp. 163–170. doi:[https://doi.org/10.1007/978-94-017-2276-6\\_18](https://doi.org/10.1007/978-94-017-2276-6_18).
- 768 Heywood, K.J., Howe, S.S., Barton, E.D., 1991. Estimation of zooplankton abundance from ship-  
borne adcp backscatter. Deep Sea Res. Part A. Oceanogr. Res. Pap. 38, 677–691. doi:[https://doi.org/10.1016/0198-0149\(91\)90006-2](https://doi.org/10.1016/0198-0149(91)90006-2).
- 770 Hitchcock, G.L., Lane, P., Smith, S., Luo, J., Ortner, P.B., 2002. Zooplankton spatial distributions  
in coastal waters of the northern arabian sea, august, 1995. Deep Sea Res. Part II Top. Stud.  
Oceanogr. 49, 2403–2423. doi:[https://doi.org/10.1016/S0967-0645\(02\)00042-5](https://doi.org/10.1016/S0967-0645(02)00042-5).
- 772 Hobbs, L., Banas, N.S., Cohen, J.H., Cottier, F.R., Berge, J., Varpe, Ø., 2021. A marine zooplankton  
774 community vertically structured by light across diel to interannual timescales. Biol. Lett. 17,  
20200810. doi:<https://doi.org/10.1098/rsbl.2020.0810>.
- 776 Hood, R.R., Beckley, L.E., Wiggert, J.D., 2017. Biogeochemical and ecological impacts of boundary  
currents in the indian ocean. Prog. Oceanogr. 156, 290–325. doi:<https://doi.org/10.1016/j.pocean.2017.04.011>.
- 780 Inoue, R., Kitamura, M., Fujiki, T., 2016. Diel vertical migration of zooplankton at the s 1  
782 biogeochemical mooring revealed from acoustic backscattering strength. J. Geophys. Res. Oceans  
121, 1031–1050. doi:<https://doi.org/10.1002/2015JC011352>.
- 784 Jadhav, S.J., Smitha, B., 2024. Abundance distribution pattern of zooplankton associated with  
the eastern arabian sea monsoon system as detected by underwater acoustics and net sampling.  
Acoust. Aust. , 1–22doi:<https://doi.org/10.1007/s40857-024-00336-w>.
- 786 Jiang, S., Dickey, T.D., Steinberg, D.K., Madin, L.P., 2007. Temporal variability of zooplankton  
788 biomass from adcp backscatter time series data at the bermuda testbed mooring site. Deep Sea  
Res. Part I Oceanogr. Res. Pap. 54, 608–636. doi:<https://doi.org/10.1016/j.dsr.2006.12.011>.

- 790 Jyothibabu, R., Madhu, N.V., Habeebrehman, H., Jayalakshmy, K.V., Nair, K.K.C., Achuthankutty, C.T., 2010. Re-evaluation of ‘paradox of mesozooplankton’ in the eastern arabian sea based on ship and satellite observations. *J. Mar. Syst.* 81, 235–251. doi:<https://doi.org/10.1016/j.jmarsys.2009.12.019>.
- 794 Kang, M., Oh, S., Oh, W., Kang, D.J., Nam, S., Lee, K., 2024. Acoustic characterization of fish and macroplankton communities in the seychelles-chagos thermocline ridge of the southwest indian ocean. *Deep Sea Res. Part II Top. Stud. Oceanogr.* 213, 105356. doi:<https://doi.org/10.1016/j.dsr2.2023.105356>.
- 798 Keerthi, M.G., Lengaigne, M., Levy, M., Vialard, J., Parvathi, V., de Boyer Montégut, C., Ethé, C., Aumont, O., Suresh, I., Akhil, V.P., Muraleedharan, P.M., 2017. Physical control of interannual variations of the winter chlorophyll bloom in the northern arabian sea. *Biogeosci.* 14, 3615–3632. doi:<https://doi.org/10.5194/bg-14-3615-2017>.
- 802 Khandagale, P.A., Mhatre, V.D., Thomas, S., 2022. Seasonal and spatial variability of zooplankton diversity in north eastern arabian sea along the maharashtra coast. *J. Mar. Biol. Assoc. India* 64, 25–32. URL: <http://mbai.org.in/php/journaldload.php?id=2618&bkid=128>.
- 806 Kidwai, S., Amjad, S., 2000. Zooplankton: pre-southwest and northeast monsoons of 1993 to 1994, from the north arabian sea. *Mar. Biol.* 136, 561–571. doi:<https://doi.org/10.1007/s002270050716>.
- 808 Kumar, S.P., Narvekar, J., 2005. Seasonal variability of the mixed layer in the central arabian sea and its implication on nutrients and primary productivity. *Deep Sea Res. Part II Top. Stud. Oceanogr.* 52, 1848–1861. doi:<https://doi.org/10.1016/j.dsr2.2005.06.002>. biogeochemical Processes in the Northern Indian Ocean.
- 812 Lawson, G.L., Wiebe, P.H., Ashjian, C.J., Gallager, S.M., Davis, C.S., Warren, J.D., 2004. Acoustically-inferred zooplankton distribution in relation to hydrography west of the antarctic peninsula. *Deep Sea Res. Part II Top. Stud. Oceanogr.* 51, 2041–2072. doi:<https://doi.org/10.1016/j.dsr2.2004.07.022>.
- 816 Lévy, M., Shankar, D., André, J.M., Shenoi, S.S.C., Durand, F., de Boyer Montégut, C., 2007. Basin-wide seasonal evolution of the indian ocean’s phytoplankton blooms. *J. Geophys. Res. Oceans* 112. doi:<https://doi.org/10.1029/2007JC004090>.
- 820 Li, M., Gargett, A., Denman, K., 2000. What determines seasonal and interannual variability of phytoplankton and zooplankton in strongly estuarine systems? *Estuar. Coast. Shelf Sci.* 50, 467–488. doi:<https://doi.org/10.1006/ecss.2000.0593>.
- 822 Liu, Y., Guo, J., Xue, Y., Sangmanee, C., Wang, H., Zhao, C., Khokattiwong, S., Yu, W., 2022. Seasonal variation in diel vertical migration of zooplankton and micronekton in the andaman sea observed by a moored adcp. *Deep Sea Res. Part I Oceanogr. Res. Pap.* 179, 103663. doi:<https://doi.org/10.1016/j.dsr.2021.103663>.

- 826 Madhupratap, M., Gopalakrishnan, T.C., Haridas, P., Nair, K.K.C., 2001. Mesozooplankton  
biomass, composition and distribution in the arabian sea during the fall intermonsoon: im-  
828 plications of oxygen gradients. Deep Sea Res. Part II Top. Stud. Oceanogr. 48, 1345–1368.  
doi:[https://doi.org/10.1016/S0967-0645\(00\)00142-9](https://doi.org/10.1016/S0967-0645(00)00142-9).
- 830 Madhupratap, M., Gopalakrishnan, T.C., Haridas, P., Nair, K.K.C., Aravindakshan, P.N., Pad-  
mavati, G., Paul, S., 1996a. Lack of seasonal and geographic variation in mesozooplankton  
832 biomass in the arabian sea and its structure in the mixed layer. Curr. Sci. 71, 863–868.  
doi:<http://drs.nio.org/drs/handle/2264/2154>.
- 834 Madhupratap, M., Haridas, P., Ramaiah, N., Achuthankutty, C.T., 1992. Zooplankton of the  
southwest coast of india: abundance, composition, temporal and spatial variability in 1987 .
- 836 Madhupratap, M., Kumar, S.P., Bhattathiri, P.M.A., Kumar, M.D., Raghukumar, S., Nair, K.K.C.,  
838 Ramaiah, N., 1996b. Mechanism of the biological response to winter cooling in the northeastern  
arabian sea. Nature 384, 549–552. doi:<https://doi.org/10.1038/384549a0>.
- 840 McCreary, J.P., Kohler, K.E., Hood, R.R., Olson, D.B., 1996. A four-component ecosystem model  
of biological activity in the arabian sea. Prog. Oceanogr. 37, 193–240. doi:[https://doi.org/10.1016/S0079-6611\(96\)00005-5](https://doi.org/10.1016/S0079-6611(96)00005-5).
- 842 McCreary, J.P., Kundu, P.K., Molinari, R.L., 1993. A numerical investigation of dynamics, ther-  
modynamics and mixed-layer processes in the indian ocean. Prog. Oceanogr. 31, 181–244.  
844 doi:[https://doi.org/10.1016/0079-6611\(93\)90002-U](https://doi.org/10.1016/0079-6611(93)90002-U).
- 846 McCreary, J.P., Murtugudde, R., Vialard, J., Vinayachandran, P.N., Wiggert, J.D., Hood, R.R.,  
Shankar, D., Shetye, S.R., 2009. Biophysical processes in the indian ocean. Indian Ocean  
Biogeochem. Processes Ecol. Variab. 185, 9–32. doi:<https://doi.org/10.1029/2008GM000768>.
- 848 Meehl, G.A., Arblaster, J.M., 2002. The tropospheric biennial oscillation and asian–australian  
monsoon rainfall. J. Clim. 15, 722–744. doi:[https://doi.org/10.1175/1520-0442\(2002\)015<0722:TTB0AA>2.0.CO;2](https://doi.org/10.1175/1520-0442(2002)015<0722:TTB0AA>2.0.CO;2).
- 850 Mooley, D.A., Parthasarathy, B., 1984. Fluctuations in all-india summer monsoon rainfall during  
1871–1978. Clim. Change 6, 287–301. doi:<https://doi.org/10.1007/BF00142477>.
- 852 Mukhopadhyay, S., Shankar, D., Aparna, S.G., Mukherjee, A., 2017. Observations of the sub-  
inertial, near-surface east india coastal current. Cont. Shelf Res. 148, 159–177. doi:<https://doi.org/10.1016/j.csr.2017.08.020>.
- 854 Nair, K.K.C., Madhupratap, M., Gopalakrishnan, T.C., Haridas, P., Gauns, M., 1999. The arabian  
sea: physical environment, zooplankton and myctophid abundance doi:<http://nopr.niscpr.res.in/handle/123456789/25690>.
- 856 Nair, P.V., 1970. Primary productivity in the indian seas. CMFRI Bulletin 22, 1–63. URL:  
858 <http://eprints.cmfri.org.in/id/eprint/610>.

- Napp, J.M., Incze, L.S., Ortner, P.B., Siefert, D.L.W., Britt, L., 1996. The plankton of shelikof  
862 strait, alaska: standing stock, production, mesoscale variability and their relevance to larval  
fish survival. Fish. Oceanogr. 5, 19–38. doi:<https://doi.org/10.1111/j.1365-2419.1996.tb00080.x>.
- Nie, L., Li, J., Wu, H., Zhang, W., Tian, Y., Liu, Y., Sun, P., Ye, Z., Ma, S., Gao, Q., 2023. The  
866 influence of ocean processes on fine-scale changes in the yellow sea cold water mass boundary  
area structure based on acoustic observations. Rem. Sens. 15, 4272. doi:<https://doi.org/10.3390/rs15174272>.
- Ohman, M.D., Hirche, H.J., 2001. Density-dependent mortality in an oceanic copepod population.  
870 Nature 412, 638–641. doi:<https://doi.org/10.1038/35088068>.
- Piontkovski, S.A., Williams, R., Melnik, T.A., 1995. Spatial heterogeneity, biomass and size struc-  
872 ture of plankton of the indian ocean: some general trends. Mar. Ecol. Prog. Ser. , 219–227URL:  
<https://www.jstor.org/stable/44634833>.
- Potiris, E., Frangoulis, C., Kalampokis, A., Ntoumas, M., Pettas, M., Petihakis, G., Zervakis, V.,  
874 2018. Acoustic doppler current profiler observations of migration patterns of zooplankton in the  
cretan sea. Ocean Sci. 14, 783–800. doi:<https://doi.org/10.5194/os-14-783-2018>.
- Prasad, T., Bahulayan, N., 1996. Mixed layer depth and thermocline climatology of the arabian sea  
878 and western equatorial indian ocean URL: <http://nopr.niscpr.res.in/handle/123456789/37119>.
- Qasim, S.Z., 1977. Biological productivity of the indian ocean doi:<http://nopr.niscpr.res.in/handle/123456789/39365>.
- Quéré, C.L., Andrew, R.M., Canadell, J.G., Sitch, S., Korsbakken, J.I., Peters, G.P., Manning,  
882 A.C., Boden, T.A., Tans, P.P., Houghton, R.A., 2016. Global carbon budget 2016. Earth Syst.  
Sci. Data 8, 605–649. doi:<https://doi.org/10.5194/essd-8-605-2016>.
- Raghukumar, S., Anil, A., 2003. Marine biodiversity and ecosystem functioning: A perspective.  
886 Curr. Sci. 84, 884–892. URL: <https://www.jstor.org/stable/24108050>.
- Ramamirtham, C.P., Murty, A.V.S., 1965. Hydrography of the west coast of india during the  
888 pre-monsoon period of the year 1962—part 2: in and offshore waters of the konkan and mal-  
abar coasts. J. Mar. Biol. Assoc. India 7, 150–168. URL: <http://eprints.cmfri.org.in/id/eprint/1579>.
- Ramamurthy, S., 1965. Studies on the plankton of the north kanara coast in relation to the  
892 pelagic fishery. J. Mar. Biol. Assoc. India 7, 127–149. URL: <http://eprints.cmfri.org.in/id/eprint/894>.
- Rehim, M., Imran, M., 2012. Dynamical analysis of a delay model of phytoplankton–zooplankton  
894 interaction. Appl. Math. Model. 36, 638–647. doi:<https://doi.org/10.1016/j.apm.2011.07.018>.

- Rippeth, T.P., Simpson, J.H., 1998. Diurnal signals in vertical motions on the hebridean shelf.  
898 Limnol. Oceanogr. 43, 1690–1696. doi:[10.4319/lo.1998.43.7.1690](https://doi.org/10.4319/lo.1998.43.7.1690).
- Ryther, J.H., Hall, J.R., Pease, A.K., Bakun, A., Jones, M.M., 1966. Primary organic production in  
900 relation to the chemistry and hydrography of the western indian ocean. Limnol. and Oceanogr. 11, 371–380. doi:<https://doi.org/10.4319/lo.1966.11.3.0371>.
- Schmidt, H., Czeschel, R., Visbeck, M., 2020. Seasonal variability of the arabian sea intermediate  
902 circulation and its impact on seasonal changes of the upper oxygen minimum zone. Ocean Sci. 16, 1459–1474. doi:<https://doi.org/10.5194/os-16-1459-2020>.
- Shankar, D., Remya, R., Anil, A.C., Vijith, V., 2019. Role of physical processes in determining  
906 the nature of fisheries in the eastern arabian sea. Prog. Oceanogr. 172, 124–158. doi:<https://doi.org/10.1016/j.pocean.2018.11.006>.
- Shankar, D., Remya, R., Vinayachandran, P.N., Chatterjee, A., Behera, A., 2016. Inhibition of  
908 mixed-layer deepening during winter in the northeastern arabian sea by the west india coastal  
910 current. Clim. Dyn. 47, 1049–1072. doi:<https://doi.org/10.1007/s00382-015-2888-3>.
- Shankar, D., Shenoi, S.S.C., Nayak, R.K., Vinayachandran, P.N., Nampoothiri, G., Almeida, A.M.,  
912 Michael, G.S., Kumar, M.R.R., Sundar, D., Sreejith, O.P., 2005. Hydrography of the eastern  
914 arabian sea during summer monsoon 2002. J. Earth Syst. Sci. 114, 459–474. doi:<https://doi.org/10.1007/BF02702023>.
- Shenoi, S.S.C., Shankar, D., Michael, G.S., Kurian, J., Varma, K.K., Kumar, M.R.R., Almeida,  
916 A.M., Unnikrishnan, A.S., Fernandes, W., Barreto, N., Gnanaseelan, C., Mathew, R., Praju,  
918 K.V., Mahale, V., 2005. Hydrography and water masses in the southeastern arabian sea during  
march–june 2003. J. Earth Syst. Sci. 114, 475–491. doi:<https://doi.org/10.1007/BF02702024>.
- Shetye, S.R., Gouveia, A.D., Shenoi, S.S.C., 1992. Does winter cooling lead to the subsurface  
920 salinity minimum off saurashtra, india? Oceanogr. Indian Ocean , 617–625URL: [http://drs.nio.org/drs/bitstream/2264/3139/2/0ceanogr\\_Indian\\_Ocean\\_1992\\_617.pdf](http://drs.nio.org/drs/bitstream/2264/3139/2/0ceanogr_Indian_Ocean_1992_617.pdf).
- Shetye, S.R., Gouveia, A.D., Shenoi, S.S.C., Michael, G.S., Sundar, D., Almeida, A.M., Santanam,  
922 K., 1991. The coastal current off western india during the northeast monsoon. Deep Sea Res. Part  
924 A. Oceanogr. Res. Pap. 38, 1517–1529. doi:[https://doi.org/10.1016/0198-0149\(91\)90087-V](https://doi.org/10.1016/0198-0149(91)90087-V).
- Shetye, S.R., Gouveia, A.D., Shenoi, S.S.C., Sundar, D., Michael, G.S., Almeida, A., Santanam,  
926 K., 1990. Hydrography and circulation off the west coast of india during the southwest monsoon  
1987 URL: [https://elischolar.library.yale.edu/journal\\_of\\_marine\\_research/1973](https://elischolar.library.yale.edu/journal_of_marine_research/1973).
- Shi, W., Wang, M., 2022. Phytoplankton biomass dynamics in the arabian sea from viirs observa-  
928 tions. J. Mar. Syst. 227, 103670. doi:<https://doi.org/10.1016/j.jmarsys.2021.103670>.
- Smeti, H., Pagano, M., Menkes, C., Dhaussy, A.L., Hunt, B.P.V., Allain, V., Rodier, M.,  
930 De Boissieu, F., Kestenare, E., Sammari, C., 2015. Spatial and temporal variability of zooplankton off n ew c aledonia (s outhwestern p acific) from acoustics and net measurements. J. Geophys. Res. Oceans 120, 2676–2700. doi:<https://doi.org/10.1002/2014JC010441>.

- 934 Smith, S., Roman, M., Prusova, I., Wishner, K., Gowing, M., Codispoti, L.A., Barber, R., Marra,  
J., Flagg, C., 1998. Seasonal response of zooplankton to monsoonal reversals in the arabian sea.  
936 Deep Sea Res. Part II Top. Stud. Oceanogr. 45, 2369–2403. doi:[https://doi.org/10.1016/S0967-0645\(98\)00075-7](https://doi.org/10.1016/S0967-0645(98)00075-7).
- 938 Smith, S.L., Madhupratap, M., 2005. Mesozooplankton of the arabian sea: patterns influenced  
by seasons, upwelling, and oxygen concentrations. Prog. Oceanogr. 65, 214–239. doi:<https://doi.org/10.1016/j.pocean.2005.03.007>.
- 942 Sreenivas, P., Patnaik, K.V.K.R.K., Prasad, K.V.S.R., 2008. Monthly variability of mixed layer  
over arabian sea using argo data. Mar. Geod. 31, 17–38. doi:<https://doi.org/10.1080/01490410701812311>.
- 944 Subrahmanyam, R., 1959. Studies on the phytoplankton of the west coast of india: Part ii. physical  
946 and chemical factors influencing the production of phytoplankton, with remarks on the  
cycle of nutrients and on the relationship of the phosphate-content to fish landings, in: Proceedings/Indian Academy of Sciences, Springer. pp. 189–252. doi:<https://doi.org/10.1007/BF03051925>.
- 948 Subrahmanyam, R., Sarma, A.H., 1960. Studies on the phytoplankton of the west coast of india.  
950 part iii. seasonal variation of the phytoplankters and environmental factors. Indian J. Fish. 7, 307–336. URL: <http://eprints.cmfri.org.in/1899/>.
- 952 Ursella, L., Cardin, V., Batistić, M., Garić, R., Gačić, M., 2018. Evidence of zooplankton vertical  
migration from continuous southern adriatic buoy current-meter records. Prog. Oceanogr. 167,  
954 78–96. doi:<https://doi.org/10.1016/j.pocean.2018.07.004>.
- 956 Ursella, L., Pensieri, S., Pallàs-Sanz, E., Herzka, S.Z., Bozzano, R., Tenreiro, M., Cardin, V.,  
Candela, J., Sheinbaum, J., 2021. Diel, lunar and seasonal vertical migration in the deep western  
958 gulf of mexico evidenced from a long-term data series of acoustic backscatter. Prog. Oceanogr. 195, 102562. doi:<https://doi.org/10.1016/j.pocean.2021.102562>.
- 960 Vijith, V., Shetye, S.R., Gouveia, A.D., Shenoi, S.S.C., Michael, G.S., Sundar, D., 2022. Circulation  
in the region of the west india coastal current in march 1994 hydrographic and altimeter data.  
J. Earth Syst. Sci. 131, 16. doi:<https://doi.org/10.1007/s12040-021-01761-5>.
- 962 Vijith, V., Vinayachandran, P.N., Thushara, V., Amol, P., Shankar, D., Anil, A.C., 2016. Con-  
sequences of inhibition of mixed-layer deepening by the west india coastal current for winter  
964 phytoplankton bloom in the northeastern arabian sea. J. Geophys. Res. Oceans 121, 6583–6603.  
doi:<https://doi.org/10.1002/2016JC012004>.
- 966 Wade, I.P., Heywood, K.J., 2001. Acoustic backscatter observations of zooplankton abundance and  
behaviour and the influence of oceanic fronts in the northeast atlantic. Deep Sea Res. Part II  
968 Top. Stud. Oceanogr. 48, 899–924. doi:[https://doi.org/10.1016/S0967-0645\(00\)00113-2](https://doi.org/10.1016/S0967-0645(00)00113-2).
- 970 Wiebe, P.H., Greene, C.H., Stanton, T.K., Burczynski, J., 1990. Sound scattering by live zooplank-  
ton and micronekton: empirical studies with a dual-beam acoustical system. The Journal of the  
Acoustical Society of America 88, 2346–2360. doi:<https://doi.org/10.1121/1.400077>.

- 972 Wiggert, J.D., Hood, R.R., Banse, K., Kindle, J.C., 2005. Monsoon-driven biogeochemical processes  
in the arabian sea. *Prog. Oceanogr.* 65, 176–213. doi:<https://doi.org/10.1016/j.pocean.2005.03.008>.
- 974
- 976 Winder, M., Schindler, D.E., 2004. Climatic effects on the phenology of lake processes. *Global  
Change Biol.* 10, 1844–1856. doi:<https://doi.org/10.1111/j.1365-2486.2004.00849.x>.
- 978
- 980 Wishner, K.F., Gowing, M.M., Gelfman, C., 1998. Mesozooplankton biomass in the upper 1000 m in  
the arabian sea: overall seasonal and geographic patterns, and relationship to oxygen gradients.  
*Deep Sea Res. Part II Top. Stud. Oceanogr.* 45, 2405–2432. doi:[https://doi.org/10.1016/S0967-0645\(98\)00078-2](https://doi.org/10.1016/S0967-0645(98)00078-2).

Table 1: ADCP deployment details at the locations. The temporal resolution is 1 hour, bin size(vertical resolution) 4 m. All ADCPs are operated at 153.3 kHz. The moorings are at a water column depth of 950–1200 m on the continental slope and are serviced on yearly basis according to ship availability. The 6th column consists of Reference echo intensity (Er) for each beam, while the 7th column contains the corresponding RSSI conversion factor (Deines, 1999).

Station (Position; °E, °N)	Date		Depth			Kc
	Deployment	Recovery	Ocean	ADCP	Er	
Okha (67.47, 22.26)	01/10/2018	01/12/2019	996	118	37 , 37 , 37 , 36	0.42 , 0.44 , 0.42 , 0.43
	01/12/2019	04/12/2020	1166	312	39 , 36 , 38 , 36	0.42 , 0.44 , 0.42 , 0.43
	04/12/2020	08/03/2022	1021	144	41 , 37 , 38 , 37	0.42 , 0.44 , 0.42 , 0.43
	08/03/2022	01/01/2023	1019	142	37 , 38 , 39 , 36	0.42 , 0.44 , 0.42 , 0.43
Mumbai (69.24, 20.01)	09/11/2017	29/09/2018	1025	150	36 , 34 , 39 , 42	0.40 , 0.40 , 0.40 , 0.40
	29/09/2018	29/11/2019	1122	125	35 , 36 , 39 , 42	0.40 , 0.40 , 0.40 , 0.40
	29/11/2019	02/12/2020	1143	164	37 , 34 , 39 , 43	0.40 , 0.40 , 0.40 , 0.40
	02/12/2020	06/03/2022	1125	142	36 , 34 , 39 , 42	0.40 , 0.40 , 0.40 , 0.40
	07/03/2022	02/01/2023	1103	158	37 , 34 , 40 , 43	0.40 , 0.40 , 0.40 , 0.40
Jaigarh (71.12, 17.53)	27/10/2017	27/09/2018	1039	198	32 , 35 , 33 , 32	0.45 , 0.45 , 0.45 , 0.45
	27/09/2018	30/10/2019	1032	164	32 , 35 , 33 , 31	0.45 , 0.45 , 0.45 , 0.45
	03/11/2019	30/11/2020	1142	264	32 , 36 , 33 , 32	0.45 , 0.45 , 0.45 , 0.45
	30/11/2020	05/03/2022	1099	119	33 , 36 , 34 , 32	0.45 , 0.45 , 0.45 , 0.45
Goa (72.74, 15.17)	03/10/2017	25/09/2018	1000	174	35 , 37 , 34 , 35	0.44 , 0.44 , 0.40 , 0.41
	25/09/2018	16/10/2019	969	145	38 , 36 , 36 , 34	0.44 , 0.44 , 0.40 , 0.41
	16/10/2019	29/11/2020	966	143	44 , 38 , 36 , 43	0.44 , 0.44 , 0.40 , 0.41
	29/11/2020	03/03/2022	985	157	35 , 40 , 35 , 38	0.44 , 0.44 , 0.40 , 0.41
	03/03/2022	05/01/2023	984	159	35 , 38 , 35 , 34	0.44 , 0.44 , 0.40 , 0.41
Udupi (74.04, 12.5)	05/10/2017	06/10/2018	1028	176	44 , 46 , 29 , 35	0.45 , 0.45 , 0.45 , 0.45
	06/10/2018	18/10/2019	1027	179	32 , 38 , 30 , 36	0.45 , 0.45 , 0.45 , 0.45
	18/10/2019	11/12/2020	1018	168	33 , 37 , 31 , 38	0.45 , 0.45 , 0.45 , 0.45
	11/03/2022	06/01/2023	1036	155	31 , 32 , 32 , 33	0.45 , 0.45 , 0.45 , 0.45
Kollam (75.44, 9.05)	07/10/2017	08/10/2018	1174	200	43 , 55 , 45 , 43	0.49 , 0.50 , 0.49 , 0.50
	08/10/2018	20/10/2019	1160	123	49 , 62 , 46 , 46	0.49 , 0.50 , 0.49 , 0.50
	20/10/2019	13/12/2020	1209	176	52 , 61 , 54 , 55	0.49 , 0.50 , 0.49 , 0.50
	13/12/2020	13/03/2022	1129	91	49 , 51 , 46 , 47	0.49 , 0.50 , 0.49 , 0.50
	13/03/2022	08/01/2023	1149	164	41 , 48 , 43 , 41	0.49 , 0.50 , 0.49 , 0.50
Kanyakumari (77.39, 6.96)	08/10/2017	10/10/2018	1055	181	32 , 34 , 38 , 35	0.45 , 0.45 , 0.45 , 0.45
	10/10/2018	22/10/2019	1075	180	36 , 34 , 39 , 36	0.45 , 0.45 , 0.45 , 0.45
	22/10/2019	14/12/2020	1060	167	33 , 35 , 36 , 35	0.45 , 0.45 , 0.45 , 0.45
	14/12/2020	14/03/2022	1184	287	34 , 36 , 36 , 35	0.45 , 0.45 , 0.45 , 0.45

Table 2:

Volumetric samples of zooplankton of various stations. The sampling depth range is standardised for later years for bin range of 0–25m, 25–50m, 50–75m, 75–100m, 100–150m. The abbreviations are in the following manner: Okha (O), Mumbai (M), Jaigarh (J), Goa (G), Udupi (U), Kollam (K), Kanyakumari (KK); The number tags corresponds to particular cruise of a station.

Sample number	Tag	Lat( $^{\circ}$ N)	Lon( $^{\circ}$ E)	Date	Time (IST)	Sampling depth range (m)
1-3	G1	15.18	72.79	25 Sep 18	452	50–25, 100–50, 150–100
4-6	G2	15.16	72.71	25 Sep 18	2108	50–25, 100–50, 150–100
7-10	G2	15.16	72.71	25 Sep 18	2137	40–20, 60–40, 80–60, 100–80
11-14	J1			26 Sep 18	2000	40–20, 60–40, 80–60, 100–80
15-17	J2			27 Sep 18	2000	50–25, 100–50, 150–100
18-21	J2			27 Sep 18	2100	40–20, 60–40, 80–60, 100–80
22-25	M1	20	69.19	28 Sep 18	2135	40–20, 60–40, 80–60, 100–80
26-27	M1	20	69.19	28 Sep 18	2205	50–25, 100–50
28-29	M2	20.01	69.2	29 Sep 18	2035	50–25, 100–50
30-33	M2	20.01	69.2	29 Sep 18	2057	40–20, 60–40, 80–60, 100–80
34-37	U1			5 Oct 18	2000	40–20, 60–40, 80–60, 100–80
38-40	U1			5 Oct 18	2100	50–25, 100–50, 150–100
41-43	U2			6 Oct 18	2000	50–25, 100–50, 150–100
44-47	U2			6 Oct 18	2100	40–20, 60–40, 80–60, 100–80
48-51	K1	9.06	75.42	8 Oct 18	421	40–20, 60–40, 80–60, 100–80
52-54	K1	9.06	75.42	8 Oct 18	449	50–25, 100–50, 150–100
55-56	K2	9.04	75.4	8 Oct 18	2027	50–25, 100–50
57-60	K2	9.04	75.4	8 Oct 18	2045	40–20, 60–40, 80–60, 100–80
61-64	G2	15.16	72.74	16 Oct 19	829	50–25, 75–50, 100–75, 150–100
65-67	G3	15.16	72.74	16 Oct 19	1812	50–25, 75–50, 100–75
68-70	K2	9.02	75.42	20 Oct 19	840	50–25, 75–50, 100–75
71-74	K3	9.04	75.43	20 Oct 19	1934	50–25, 75–50, 100–75, 150–100
75-78	KK1			22 Oct 19	742	50–25, 75–50, 100–75, 150–100
79-82	KK2			22 Oct 19	1925	50–25, 75–50, 100–75, 150–100
83-86	J1			30 Oct 19	324	50–25, 75–50, 100–75, 150–100
87-89	J2			4 Nov 19	946	75–50, 100–75, 150–100
90-92	M2	19.98	69.22	29 Nov 19	1434	50–25, 75–50, 100–75
93-96	M3	20.01	69.23	30 Nov 19	958	50–25, 75–50, 100–75, 150–100
97-100	O1	22.24	67.49	1 Dec 19	937	50–25, 75–50, 100–75, 150–100
101	O2	22.25	67.46	1 Dec 19	1957	150–100
102-105	G3	15.68	73.22	28 Nov 20	930	50–25, 75–50, 100–75, 150–100
105-108	G4	15.32	73.22	29 Nov 20	1558	50–25, 75–50, 100–75, 150–100
108-110	J2	17.85	71.21	30 Nov 20	1458	75–50, 100–75, 150–100
111-114	J3	17.91	71.21	1 Dec 20	1052	50–25, 75–50, 100–75, 150–100
115-118	M4	20.03	69.38	2 Dec 20	2016	50–25, 75–50, 100–75, 150–100
119.00	O2	22.41	67.8	4 Dec 20	953	150–100
120-123	O3	22.41	67.79	4 Dec 20	2011	50–25, 75–50, 100–75, 150–100
124-127	K3	9.11	75.72	12 Dec 20	2335	50–25, 75–50, 100–75, 150–100
128-131	K4	9.06	75.74	13 Dec 20	1507	50–25, 75–50, 100–75, 150–100
132-134	KK1	7.62	77.63	14 Dec 20	1226	50–25, 75–50
135-138	KK2	7.62	77.63	14 Dec 20	2047	50–25, 75–50, 100–75, 150–100
139-142	G4	15.32	73.21	3 Mar 22	823	50–25, 75–50, 100–75, 150–100
143-146	G5	15.68	73.21	4 Mar 22	1030	50–25, 75–50, 100–75, 150–100
147-150	M5	19.99	69.23	7 Mar 22	957	50–25, 75–50, 100–75, 150–100
151-154	O3	22.24	67.5	8 Mar 22	806	50–25, 75–50, 100–75, 150–100
155-158	U3	12.5	74.04	12 Mar 22	1156	50–25, 75–50, 100–75, 150–100
159-160	K4	9.04	75.42	13 Mar 22	1027	50–25, 75–50, 100–75
161-164	KK3	6.97	77.4	15 Mar 22	1220	50–25, 75–50, 100–75, 150–100

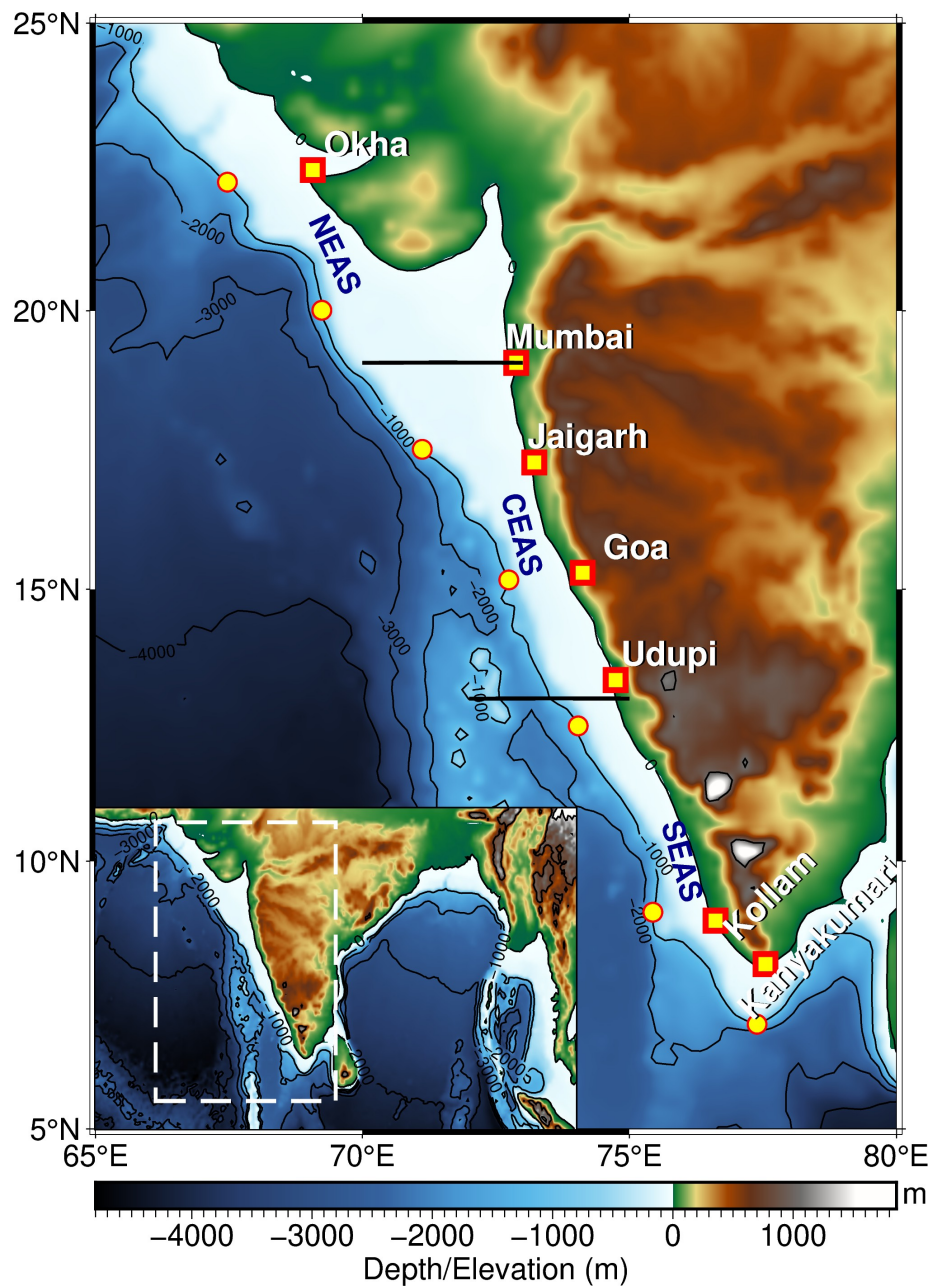


Figure 1: Map showing region of interest in eastern Arabian Sea. The slope moorings are deployed at  $\sim 1000$  m depth as shown in the bathymetry contour. Note the increase in shelf width as we go poleward along the coast. The mooring sites off Okha and Mumbai are in NEAS; Jaigarh and Goa in CEAS while Kollam and Kanyakumari are at SEAS. Udupi is situated at the transition zone of CEAS and SEAS.

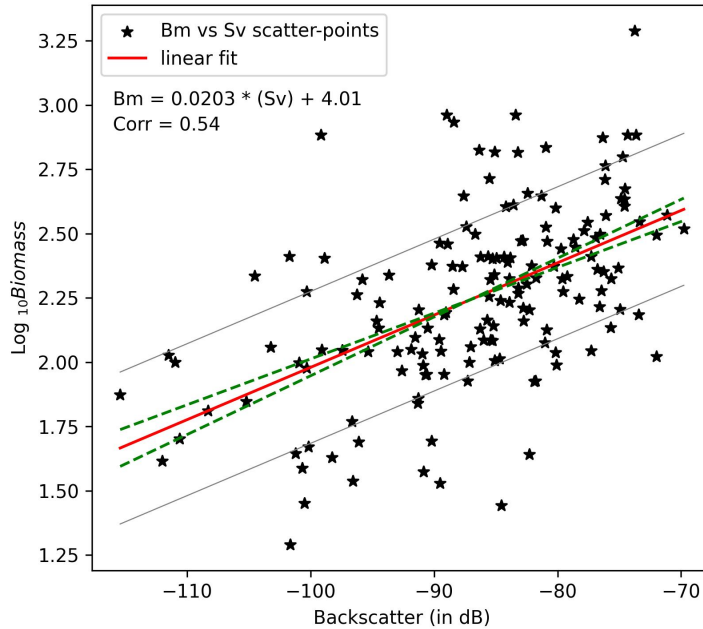


Figure 2: Linear regression of biomass ( $\log_{10}$  scale) and backscattering strength (in dB) is shown. The linear fit line is within the error range of previous result of (Aparna et al., 2022) (contained 67 data points) onto which latest zooplankton volumetric sample data (159 data points) is appended. The regression equation is  $y = (0.02 \pm 0.0025) x + (4.0144 \pm 0.2198)$  and correlation value of 0.54. The dashed green lines denote error range of plausible slope and intercept. From the linear equation, the upper and lower bound of error limit leads to an error bar of  $\sim 14 \text{ mg m}^{-3}$ . Standard deviation ( $\sigma$ ) of  $\log_{10}(\text{Biomass})$  is  $\pm 0.49$ , which results in the backscatter range of 48.58 dB encompassing the entire backscatter range. It signifies the robustness of zooplankton biomass dependency on ADCP measured backscattering strength.

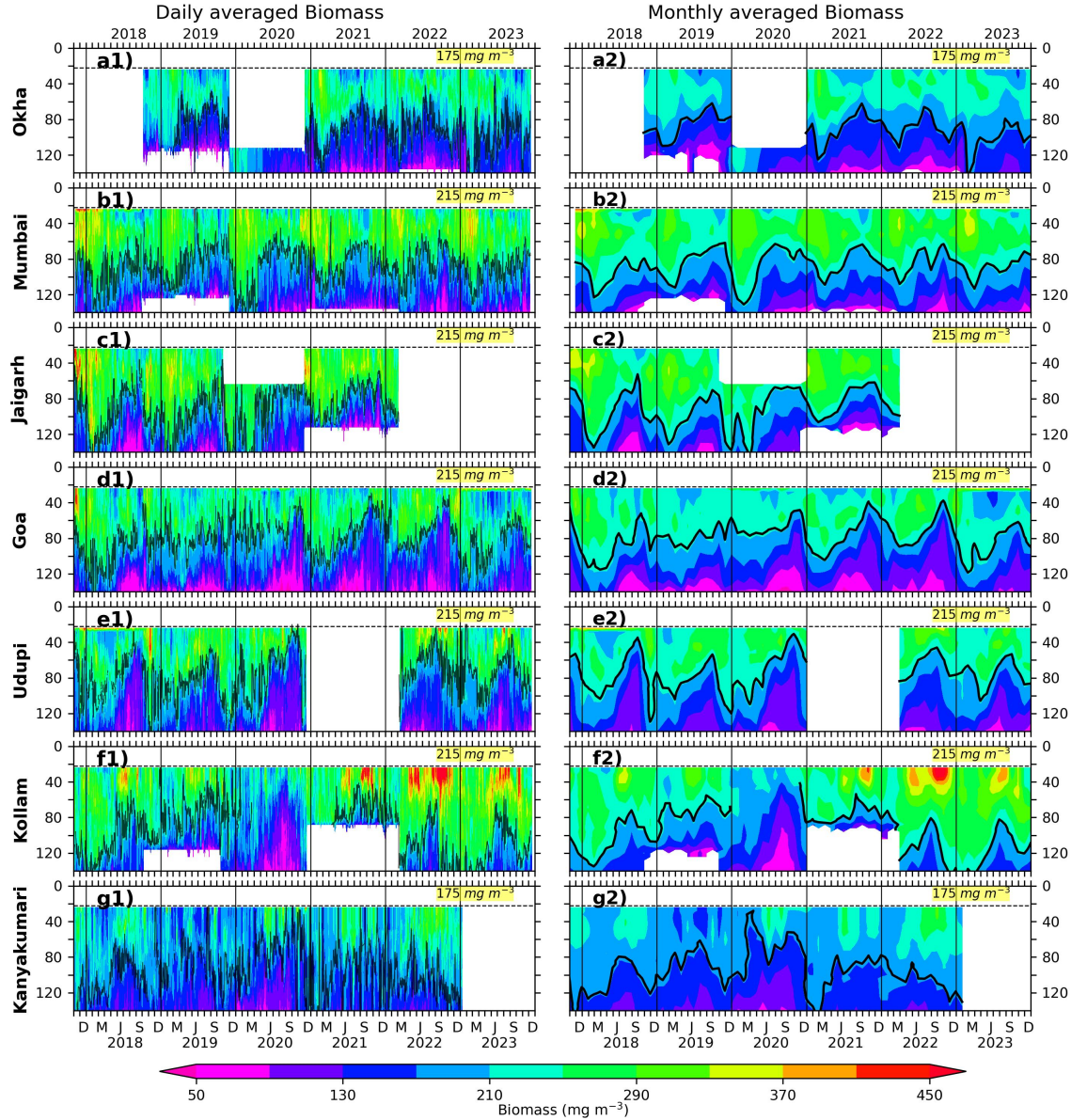


Figure 3: Daily and monthly averaged biomass for EAS moorings, north (top) to south (bottom). The black contours are marking of  $175 \text{ mg m}^{-3}$  biomass for Okha and Kanyakumari;  $215 \text{ mg m}^{-3}$  for rest of the locations namely. The biomass contours are distinct and different based on the physico-chemical parameters and these are the one that best explains seasonality at respective location. The top 10% of data is discarded due to echo noise. The dashed line at 22 m marks the top-depth of first bin i.e, 24 m, vertical black lines separates years. During 2020 off Kollam, a lack of suitable biomass contour to show seasonality is due to strong interannual variations.

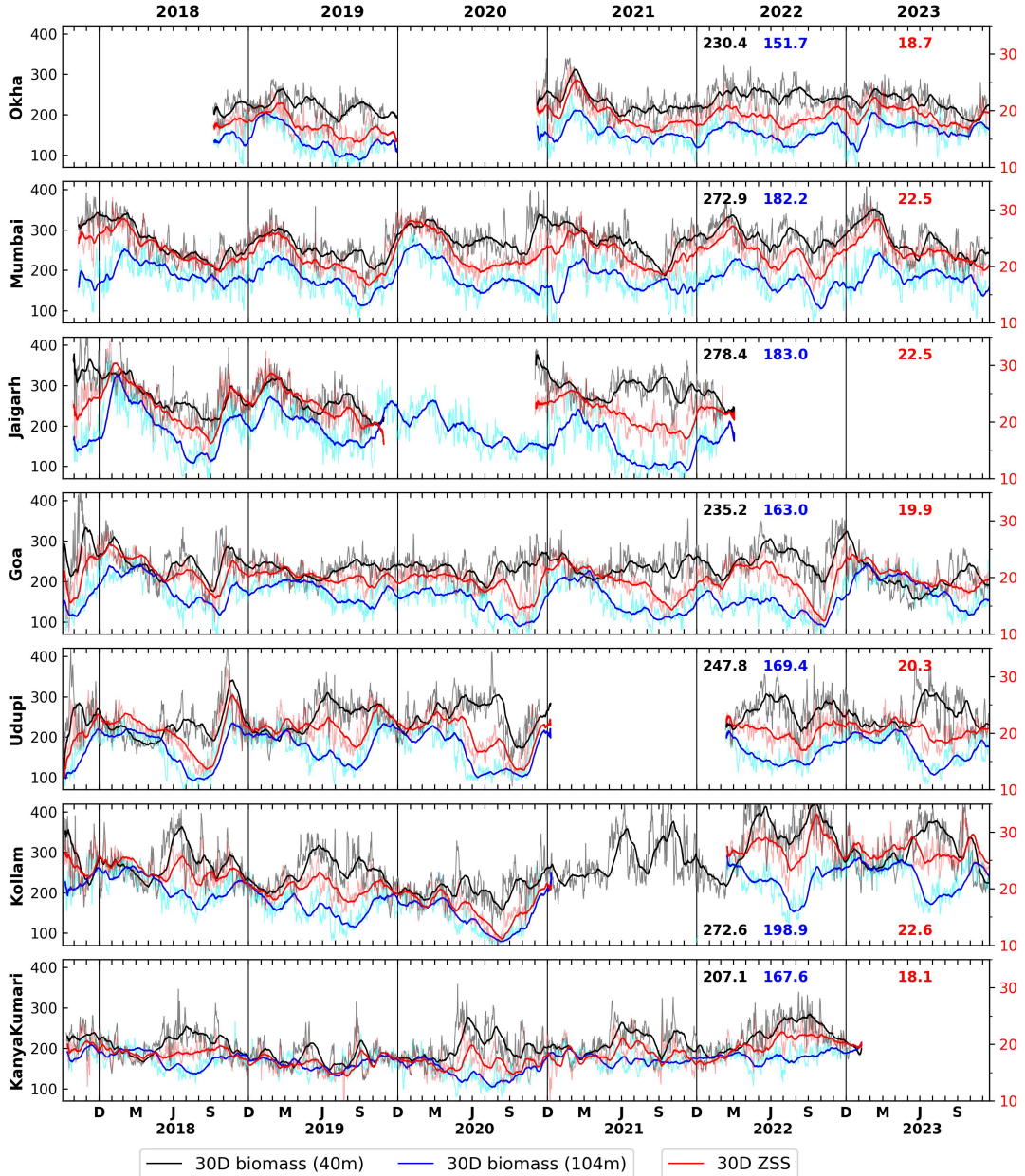


Figure 4: The biomass at depth of 40 m (grey, black) and 104 m (cyan, blue) and ZSS (pink, red, 24–120 m biomass integral), the lighter (darker) shades shows daily (30 day rolling averaged) sample, respectively. The mean biomass at 40 and 104 m, and mean ZSS is shown on top right corner in corresponding color. Notice the spikes (bursts) seen in the daily (rolling mean) data of biomass at 40 m that lasts few days (few days to weeks), e.g., during many isolated days of June of 2020 (during entire June–July of 2020) off SEAS. These spikes and bursts are seen at all locations, at 40 and 104 m, albeit with a varied magnitude.

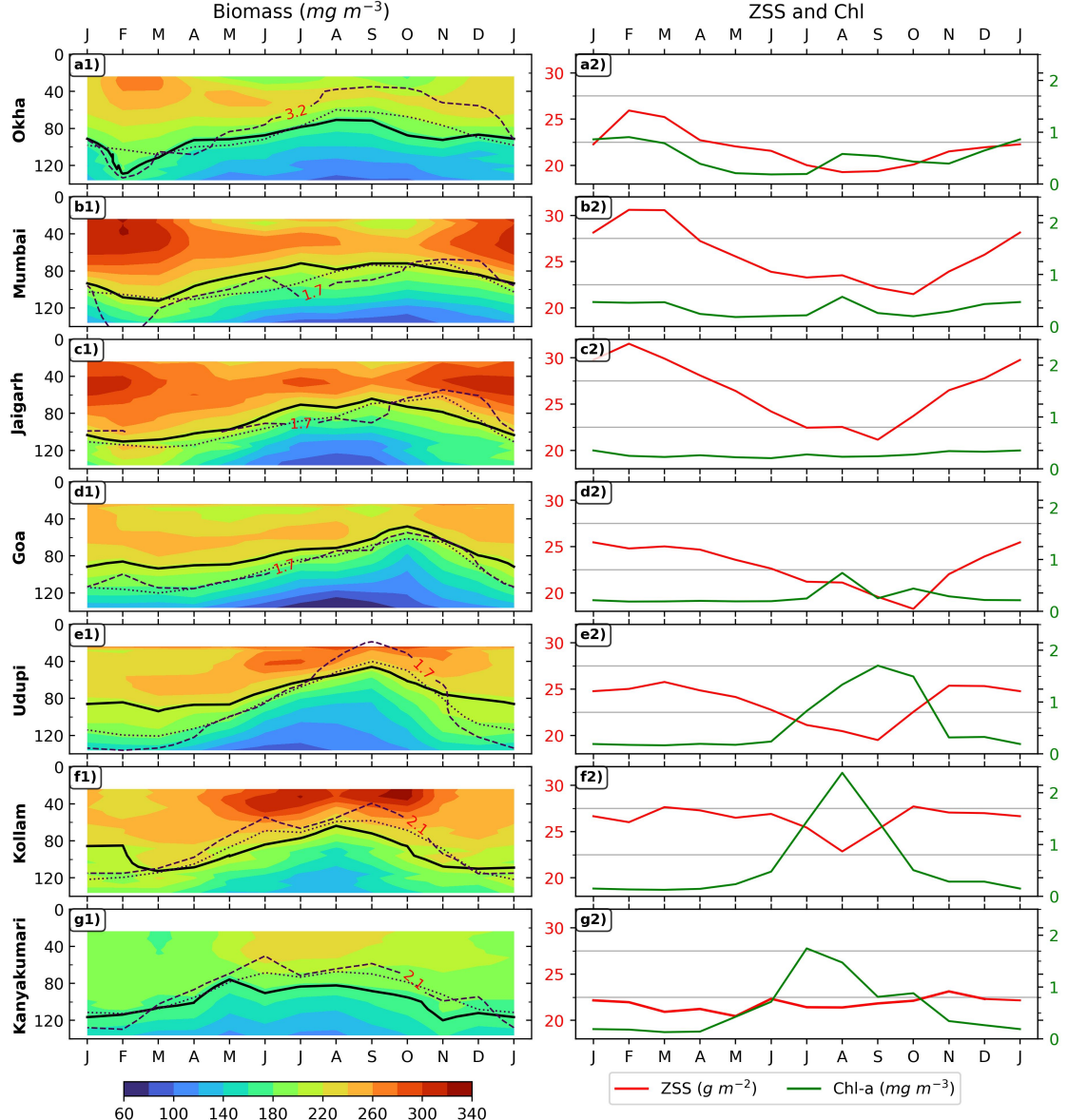


Figure 5: Monthly climatology of zooplankton biomass is shown in left panels for seven locations. The D175 and D215 are shown in solid lines; dashed line represents the depth of 23°C isotherm; oxygen contours are shown in dotted lines and labeled for each mooring. The right set of panel plots is showing ZSS (24–140 biomass integral) and chl-a climatology for corresponding locations.

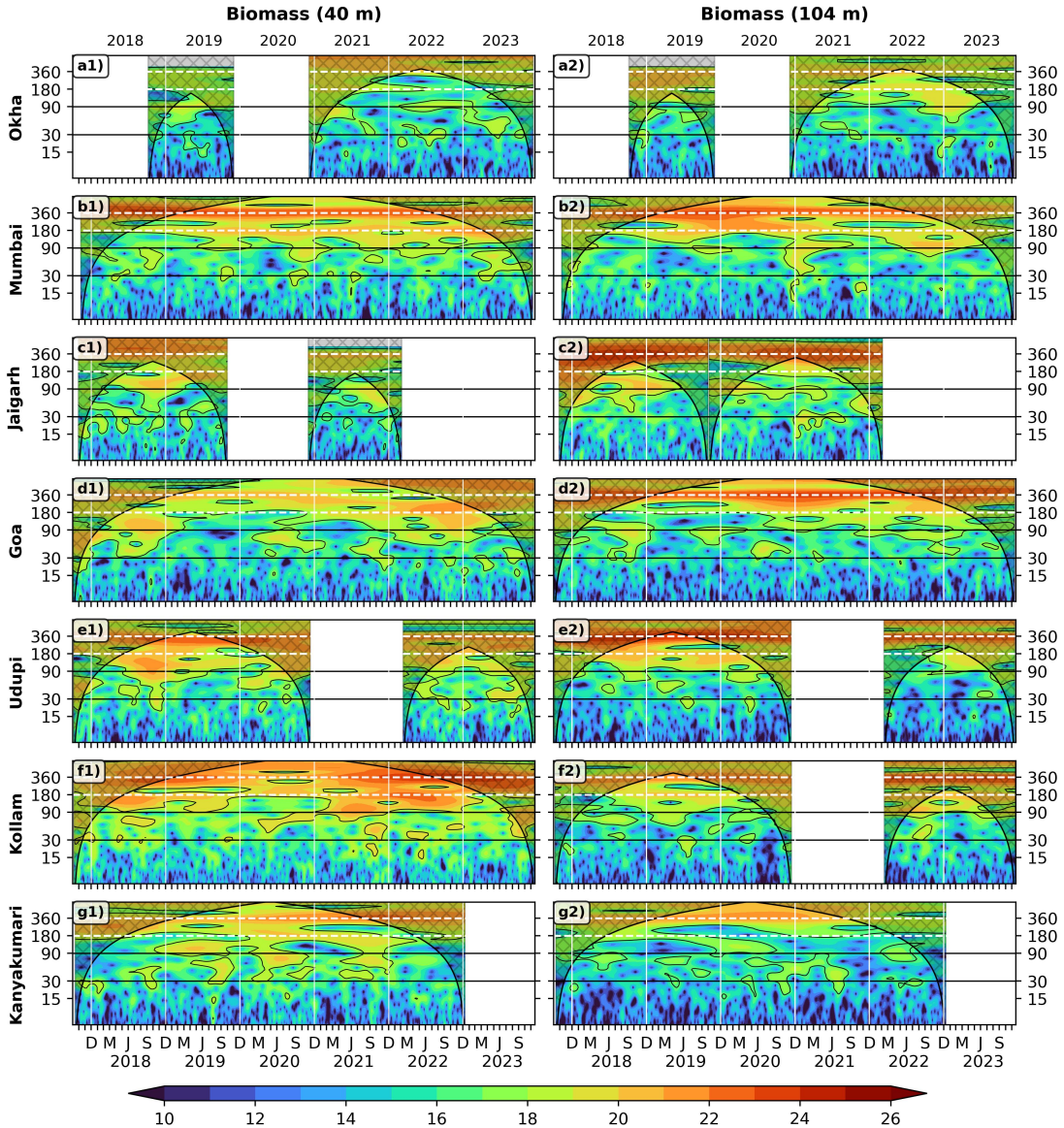


Figure 6: Wavelet power spectra (morlet) of the 40 m (left panel) and 104 m (right panel) zooplankton biomass plotted against time as abscissa and period in days as ordinate. The wavelet power is in  $\log_2$  scale, the 95% significance is marked in black contours; the cross-shaded region falls under cone of influence. The horizontal dashed white (solid black) lines shows annual and semi-annual periods (intraseasonal band), vertical white lines separates years.

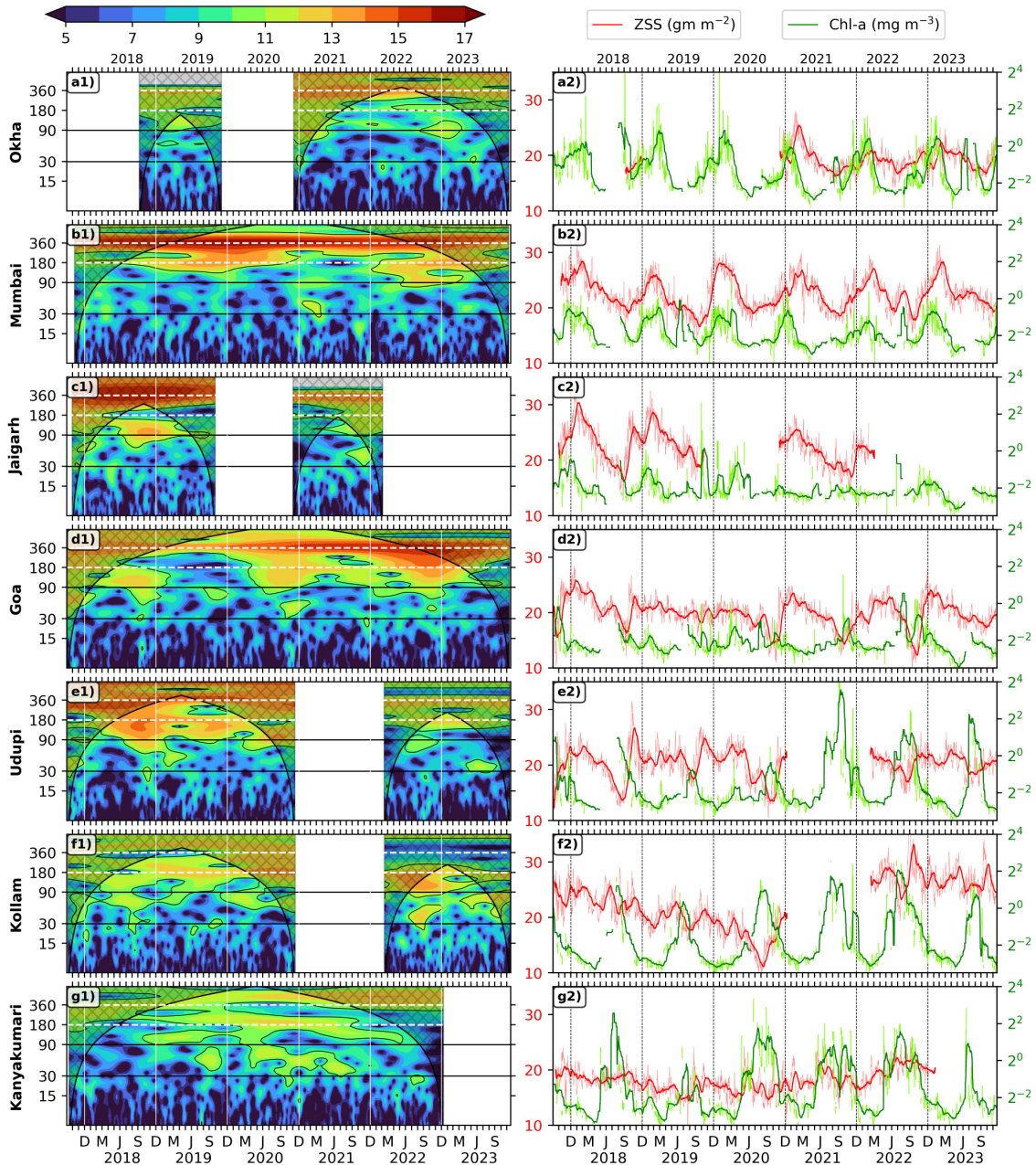


Figure 7: Wavelet power spectra of ZSS plotted against time as abscissa and period in days as ordinate in left panel. The wavelet power is in log<sub>2</sub> scale, the 95% significance is marked in black contours; The vertical white lines separates years. The right side panel shows the ZSS (24–120 m biomass integral) time series of 30 day rolling mean data (red) overlaid upon daily data (pink). The 30 day rolling mean data of chl-a (solid green) is plotted over its daily data (light green).

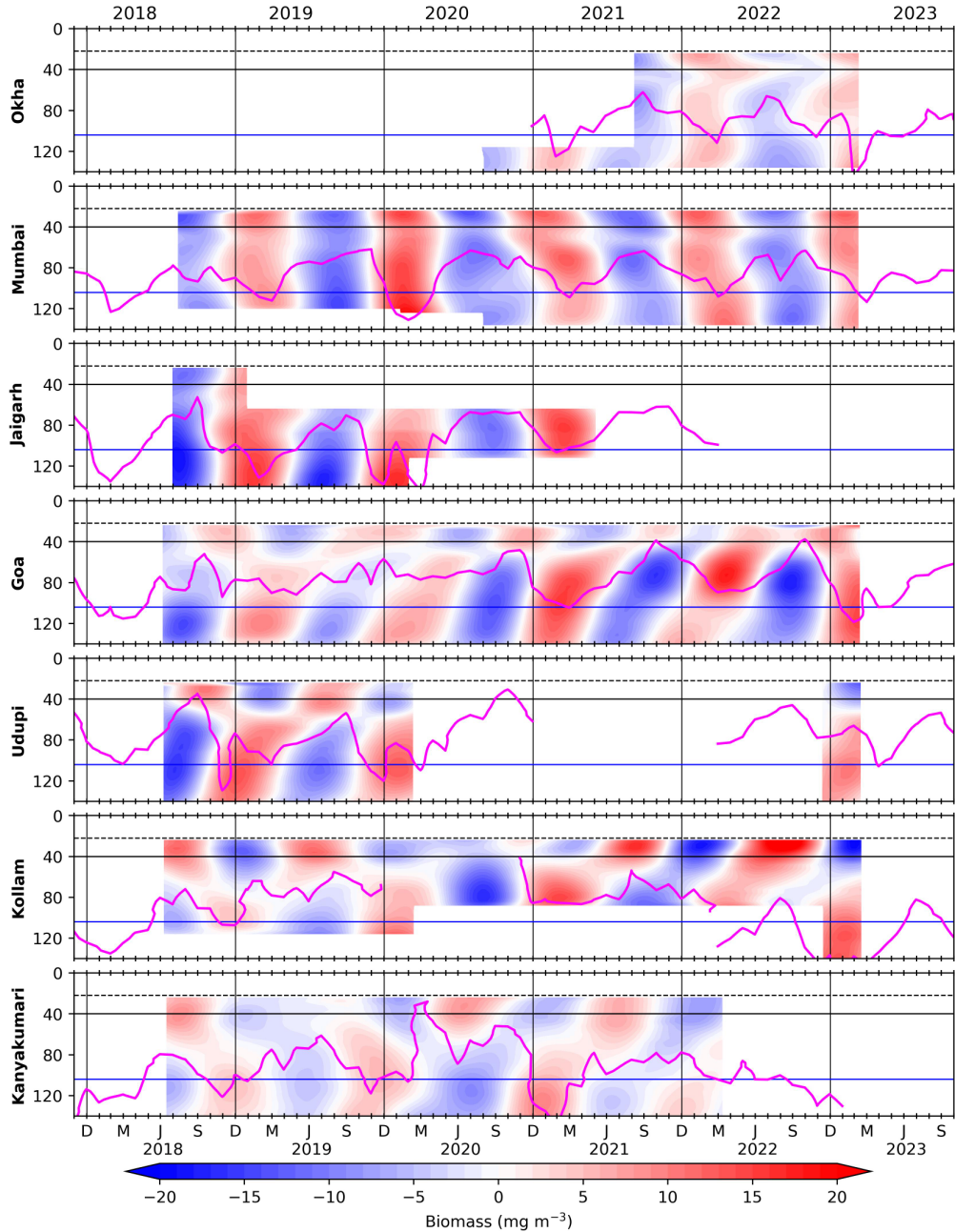


Figure 8: The biomass variation occurring in annual band (300 to 400 days). Owing to the presence of seasonal reversal of current, there is a variation driven by associated upwelling (downwelling) processes in summer (winter) monsoon. The horizontal black and blue lines is for 40 and 104 m; vertical black lines separate the years. The dashed line at 22 m marks the top-depth of first bin i.e, 24 m and solid magenta curves denotes D215 (D175 off Okha and Kanyakumari) fetched from monthly biomass.

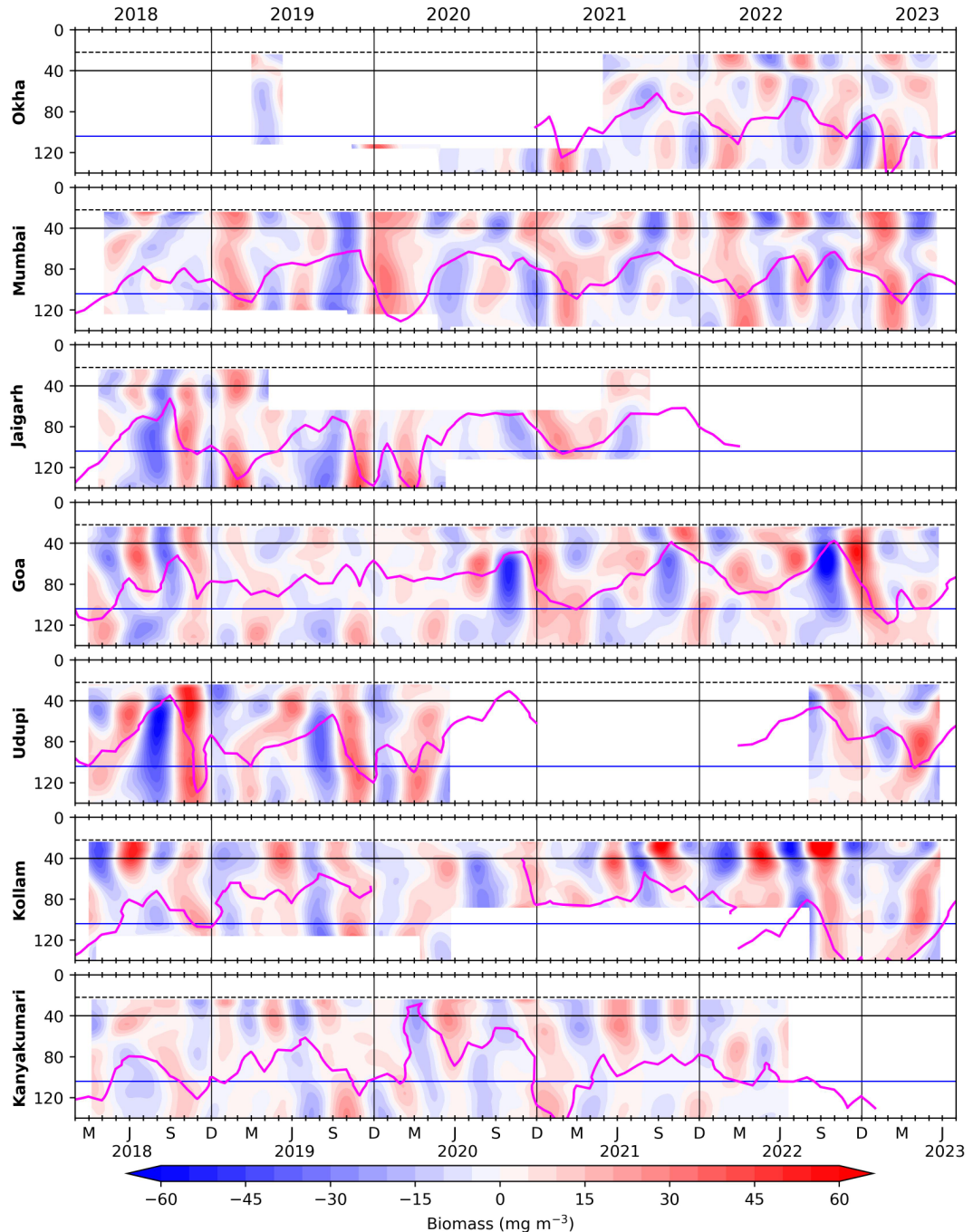


Figure 9: The biomass variation occurring in 100 to 250 days period (between the seasons and within a year record or intra-annual band) is obtained using a band pass filter. The horizontal black and blue lines is for 40 and 104 m, vertical black lines separate the years. Dashed line at 22 m marks the top-depth of first bin i.e, 24 m and solid magenta curves denotes D215 (D175 off Okha and Kanyakumari) obtained from monthly biomass time series.

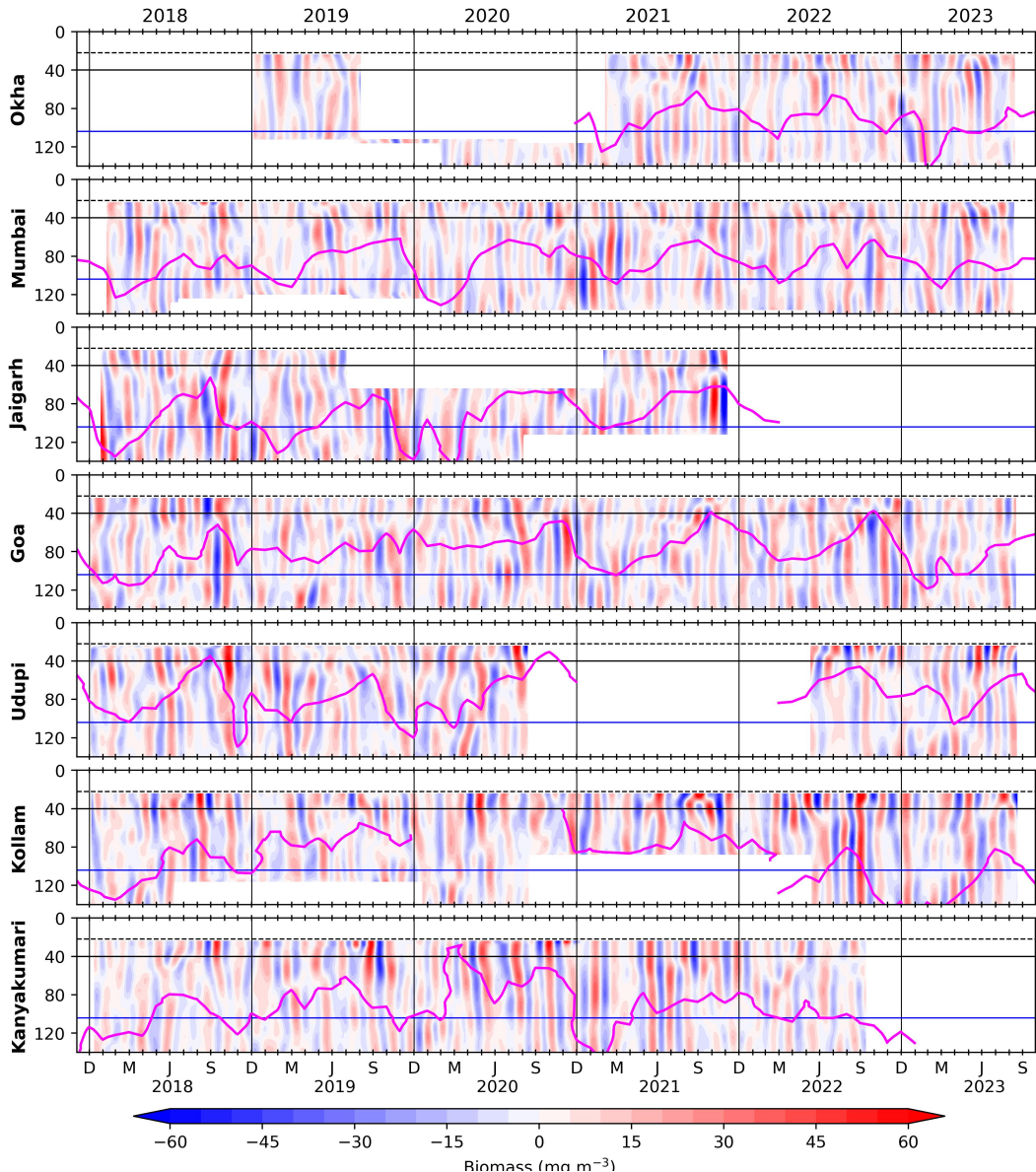


Figure 10: Biomass variation in intraseasonal band i.e., 30 to 90 days period is obtained using a lanczos band pass filter. The horizontal black and blue lines is for 40 and 104 m, vertical black lines separate the years and solid magenta curves denotes D215 (D175 off Okha and Kanyakumari) fetched from monthly biomass. The dashed line at 22 m marks the top-depth of first bin i.e, 24 m. Intraseasonal variability is seen throughout the record, and it is coherent along the slope and its magnitude is stronger during August to November.

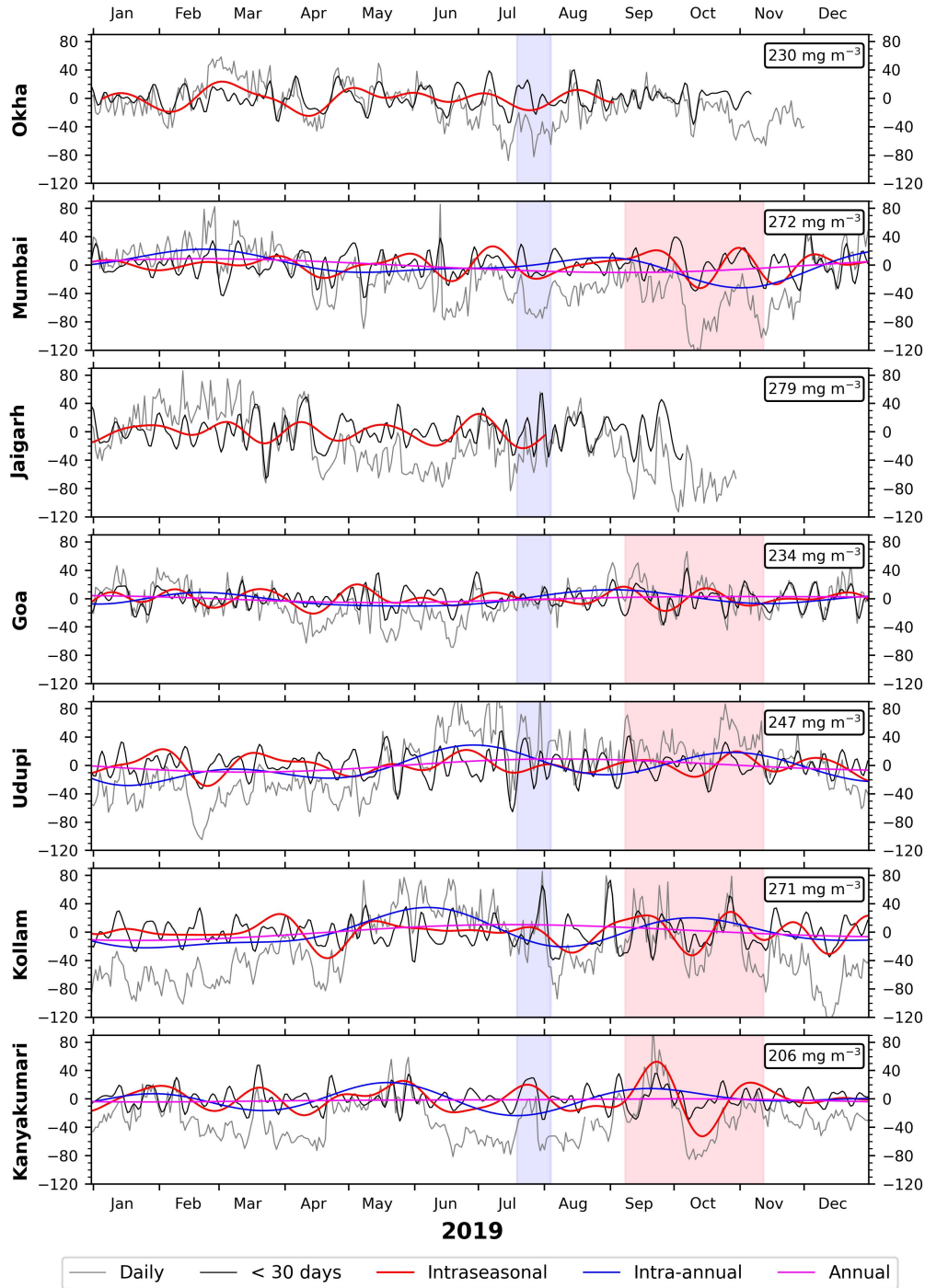


Figure 11: Comparison between mean-removed daily biomass time series at 40 m and the distinct variability components all locations for 2019. The biomass units are  $\text{mg m}^{-3}$  and its mean for respective location is shown in top right box. Off Mumbai and Kollam, an increase in biomass is noticed from May onward lasting till late monsoon with weeks of low biomass during August due to low contribution of intraseasonal component of variability. The pink (blue) shade has a span of  $\sim 65$  days ( $\sim 15$  days), and it highlights regions showing coherence in 30–90 days (5–30 days) of intraseasonal band. The stand-alone spikes are representative of patchiness i.e., dense clusters of zooplankton and may not necessarily be observed elsewhere. Annual variability is very weak and lies close to zero almost always.